UAV Swarm Position Optimization for High Capacity MIMO Backhaul

Samer Hanna, *Graduate Student Member, IEEE*, Enes Krijestorac, *Graduate Student Member, IEEE*, and Danijela Cabric, *Fellow, IEEE*

***Abstract*— A swarm of cooperating UAVs communicating with a distant multiantenna ground station can leverage MIMO spatial multiplexing to scale the capacity. Due to the line-of-sight propagation between the swarm and the ground station, the MIMO channel is highly correlated, leading to limited multiplexing gains. In this paper, we optimize the UAV positions to attain the maximum MIMO capacity given by the single user bound. An infinite set of UAV placements that attains the capacity bound is first derived. Given an initial swarm placement, we formulate the problem of minimizing the distance traveled by the UAVs to reach a placement within the capacity maximizing set of positions. An offline centralized solution to the problem using block coordinate descent is developed assuming known initial positions of UAVs. We also propose an online distributed algorithm, where the UAVs iteratively adjust their positions to maximize the capacity. Our proposed approaches are shown to significantly increase the capacity at the expense of a bounded translation from the initial UAV placements. This capacity increase persists when using a massive MIMO ground station. Using numerical simulations, we show the robustness of our approaches in a Rician channel under UAV motion disturbances.**

***Index Terms*— Unmanned aerial vehicle, MIMO, cooperative communication.**

I. Introduction

DRIVEN by their low cost, high mobility, and ease of deployment, unmanned aerial vehicles (UAVs) are used in many applications including delivery of goods, surveillance, precision agriculture, and civil infrastructure inspection [1]. For wireless communications, UAVs have been proposed as aerial basestations (BS) [2], data aggregators [3], and for many other applications [4]. The key advantage of UAV deployments over ground antennas is their mobility [4]. By changing the position of UAVs, the wireless communications channel can be designed to be a line-of-sight channel for a given deployment [5]. However, unlike ground BSs which rely on wired communications for backhaul, UAV backhaul has to be wireless, which makes it one of the challenges of UAV BSs [6]. In scenarios requiring high throughput like open-air festivals [7, Sec. 15], multiple UAVs need to be deployed due to the lack of nearby fixed infrastructure. In such multi-UAV deployments, the UAVs are positioned close to the ground users, yielding a high SNR access link. In contrast, the backhaul link with a distant ground station has lower SNR and is shared among multiple UAVs thus creating a bottleneck for communications.

Using a multiantenna ground station (GS) makes the backhaul air-to-ground channel between the swarm of UAVs and the GS a MIMO channel. By leveraging spatial multiplexing in this channel, the backhaul capacity can significantly be improved. However, the air-to-ground channel between a UAV swarm and the GS is typically dominated by line-of-sight (LOS) propagation [8]. Additionally, the GS antenna array is typically implemented as a uniform linear or rectangular array with limited dimensions. These factors can lead to highly correlated low-rank channels that can limit the MIMO capacity gains [9, Sec. 7.2.3]. Optimizing the UAV swarm positions can reduce the channel correlation and improve capacity. But, this optimization for backhaul capacity should have a minimum impact on the UAV deployment application.

The concept of positioning antennas to optimize the MIMO channel was first proposed for LOS communications between fixed GSs. By optimizing the spacing of uniform antenna arrays, the maximum capacity given by the single user bound can be achieved [10]. Once synchronized [11], a cooperative UAV swarm can be viewed as a virtual antenna array. But unlike GSs, which are limited in size and typically consist of uniformly spaced antenna elements, UAV swarms can achieve large apertures and are not bound to any geometry. This flexibility allows a swarm to maximize the backhaul capacity at the cost of moving the UAVs from their initial positions [12]. While it is possible to optimize for access and backhaul link simultaneously [13], this limits the scope of the problem to UAV BSs. Communications intensive UAV applications tolerating some displacement are numerous and can include some video surveillance and remote sensing deployments [1].

In this paper, for a communications intensive application, we optimize the placements of UAVs within a swarm to attain the maximum MIMO capacity over a backhaul link with a distant uniform rectangular GS. Using the GS geometry and the LOS channel, we derive a set of UAV positions that attain the maximum capacity given by the single user bound.

Manuscript received October 15, 2020; revised February 21, 2021; accepted April 11, 2021. Date of publication June 16, 2021; date of current version September 16, 2021. This work was supported in part by the NSF under Grant 1929874 and in part by the CONIX Research Center, one of six centers in JUMP through the Semiconductor Research Corporation (SRC) Program sponsored by the DARPA. *(Corresponding author: Samer Hanna.)*

The authors are with the Department of Electrical and Computer Engineering, University of California at Los Angeles, Los Angeles, CA 90095 USA (e-mail: samerhanna@ucla.edu; enesk@g.ucla.edu; danijela@ee.ucla.edu).

Color versions of one or more figures in this article are available at https://doi.org/10.1109/JSAC.2021.3088677.

Digital Object Identifier 10.1109/JSAC.2021.3088677

0733-8716 © 2021 IEEE. Personal use is permitted, but republication/redistribution requires IEEE permission.
See https://www.ieee.org/publications/rights/index.html for more information.

Authorized licensed use limited to: ASU Library. Downloaded on August 18,2023 at 20:13:23 UTC from IEEE Xplore. Restrictions apply.

Among the capacity maximizing position set, UAV positions closer to their initial placements pose the least disturbance to the deployment application and are desirable. Based on that, we formulate the problem of finding the positions within the capacity maximizing set that minimize the traveled distance from the initial positions. Two methods are considered to solve this problem; the first one is a centralized offline solution assuming a prior knowledge of the UAVs' initial positions. The second approach is a distributed online approach, where the UAVs iteratively adjust their positions to maximize the backhaul capacity. Our contributions are

- We show that, for a uniform rectangular array ground station, the set of UAV placements maximizing the MIMO capacity is infinite. We derive a subset of placements within this set in the far-field where the distance from the swarm to the ground station is much larger than the size of the swarm.
- Given the UAVs' initial placements, we formulate the problem of finding UAV positions within the capacity maximizing set that minimize the distance traveled. A centralized suboptimal solution to this problem using block coordinate descent is developed and shown to require a bounded traveled distance per UAV.
- An online distributed algorithm is proposed to maximize the capacity, requiring only sharing of channel estimates between neighboring UAVs. The conditions needed to guarantee its convergence and an upper bound for the traveled distance are derived.

II. Related Work

Many of the existing works have focused on optimizing the UAV positions to improve only the access link [2], [14], [15], thus implicitly assuming an ideal backhaul link. However, as the number of UAVs increase, wireless backhaul becomes challenging [6]. Some works have proposed different approaches for UAV backhaul which we briefly discuss. We also discuss MIMO in UAV networks; some works has envisioned massive MIMO BS serving UAVs, others have proposed multiantenna UAV BSs. Swarms of single antenna UAVs were also proposed communicating with either ground users or GSs.

A. Approaches for UAV Backhaul

To address the challenges associated with UAV wireless backhaul, several approaches were proposed in the literature. Some works have proposed using mmWave backhaul [16], [17], however, the high path loss at these frequencies makes them unsuitable for long links. Mechanical antenna steering was proposed for UAVs backhaul at microwave frequencies [18], but mechanical steering limits beamforming to one direction and is inherently slower. Integrated access and backhaul (IAB) links optimization was proposed in [13], [19], [20], where UAVs relay data using the same frequency bands in both links. In [19], the locations, power allocation, and frequency assignment of a swarm of UAVs were optimized to reduce the transmit power in an IAB network using a single antenna GS. The UAVs' frequency assignment is chosen to minimize the interference between the backhaul and access links, which share the same bands. In [20], using IAB, exhaustive search is used to determine the UAV locations, precoder design, power allocations, which maximize the sum-rate to the ground users using a massive MIMO GS for backhaul. However, due to the prohibitive complexity of exhaustive search, only one UAV was considered. A less complex centralized solution to the same problem using a fixed point method and particle swarm optimization was proposed in [13]. Results have shown that increasing the number of UAVs increases the interference in the access link and reduces the network performance. In IAB networks, the main challenge is to minimize the interference in the access link and between both access and backhaul links since the same frequencies are reused. In this paper, our focus is on maximizing the swarm MIMO backhaul capacity for any application tolerating displacement from a given initial placement. In the case of UAV BSs, the access link is assumed to use a different frequency band than the backhaul link.

B. UAVs Served by Massive MIMO BS

In [21], [22], massive MIMO cellular BSs were proposed for cellular-connected UAVs and are shown to improve the data rates. Unlike our work, the UAVs are treated as user equipment with no control over their positions. Deep reinforcement learning was also proposed for navigation of a single UAV communicating with a massive MIMO BS in [23]. The impact of having a swarm of UAVs on the capacity was not considered.

C. MIMO Using Multiantenna UAVs

Using UAVs carrying antenna arrays was proposed in many works in the literature. Some works have considered optimizing the positions and the beamforming vectors to improve the ground users' SNR [24] or minimize the transmit power [25]. The trajectory of multiantenna UAVs serving ground users under an uncertain environment was optimized in [26]. However, for UAVs carrying an antenna array, the UAV size and maximum payload for safe flight significantly constrains the antenna array aperture compared to a swarm of single antenna UAVs, thus limiting the multiplexing gains with a distant GS.

D. MIMO Using UAV Swarms

Several existing works have proposed UAV swarms leveraging MIMO. These works have either considered the access link with ground users or the backhaul link with a GS. For the access link, in [27], the motion and beamforming weights of linearly arranged UAV swarm were optimized to serve users one at a time. To serve multiple ground users simultaneously, UAVs were proposed as remote radio heads in a coordinated multipoint (CoMP) system and were optimized to improve the capacity in [28] and physical layer security in [29]. Access link air to ground channel is different from the backhaul channel; in the former, the ground users are typically spread out, closer to the UAVs, and are more likely to get obstructed unlike a distant GS with a dominant LOS channel in the latter.

To improve the capacity in LOS channels, before the interest in UAV networks, the designs of traditional uniform antenna

Authorized licensed use limited to: ASU Library. Downloaded on August 18,2023 at 20:13:23 UTC from IEEE Xplore. Restrictions apply.

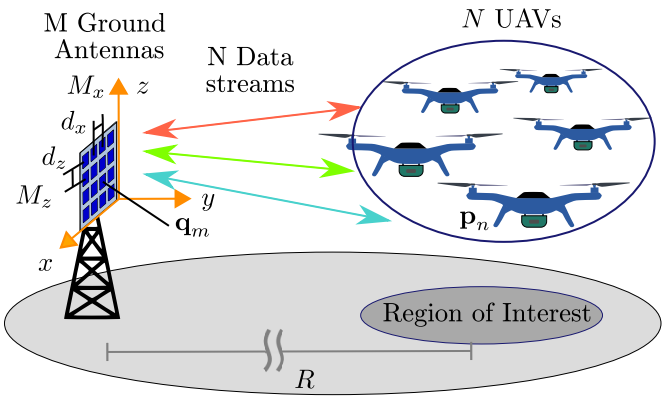

Fig. 1. In the proposed system model, the UAV swarm is in the far-field of a uniform rectangular antenna array GS.

arrays like linear and rectangular were optimized in [30], [31]. Based on these designs, uniform geometries were proposed for UAV swarms communicating with GS in [32]–[34]. However, these rigid geometrical placements might conflict with positions required by application-driven deployments. In [35], for a given UAV deployment, the massive MIMO GS was optimized to maximize the ergodic LOS channel capacity, thus not benefiting from the UAVs mobility and requiring GS redesign per deployment. In [36], the authors proposed randomly placing the UAVs within a specified area for optimal MIMO capacity. Due to the randomness of this approach, the capacity improvements are probabilistic and a large capacity increase requires having more UAVs than GS antennas. In [12], two iterative distributed algorithms were proposed to optimize the LOS MIMO channel capacity of a UAV swarm; namely gradient descent and brute force, which are described later in this work. However, no convergence proofs nor travel upper bounds were developed for the proposed algorithms. In this work, we leverage the UAV mobility to optimize the backhaul link capacity. Our proposed approaches minimize the UAVs' displacements from given initial positions. Upper bounds on the distance traveled and convergence proofs are derived for our proposed approaches.

III. System Model

A swarm of N single antenna UAVs is communicating with a multiantenna GS having M antennas in either uplink or downlink. Each UAV has its own data to transmit or to receive. To avoid high inter-swarm communications overhead, the MIMO processing (precoding for downlink and combining for uplink) is done at the GS and each UAV sends or receives only its own stream. Since the maximum number of simultaneous streams possible is $\min(M, N)$, at most $N = M$ UAVs can benefit from the MIMO gains. Hence, throughout this work, we assume that $N \leq M$. If $N > M$, time multiplexing or another technique has to be used, which is not considered in this work.

The channel between the swarm and the ground antennas can be modeled as a Rician channel [8] and is denoted by $\mathbf{H} \in \mathbb{C}^{M \times N}$ defined as follows [30]

$$\mathbf{H} = \sqrt{\frac{K}{K+1}}\mathbf{H}_{\text{LOS}} + \sqrt{\frac{1}{K+1}}\mathbf{H}_{\text{NLOS}} \tag{1}$$

where K is the K-factor, $\mathbf{H}_{\text{LOS}}$ is the line-of-sight (LOS) component and $\mathbf{H}_{\text{NLOS}}$ is the non-line-of-sight (NLOS) component. The elements of $\mathbf{H}_{\text{NLOS}}$ are independently drawn from a zero-mean circularly symmetric complex Gaussian distribution with variance equal to $\frac{\|\mathbf{H}_{\text{LOS}}\|_F}{MN}$,where $\|.\|_F$ is the Frobenius norm. The normalized LOS channel $\overline{\mathbf{H}}_{\text{LOS}}$ and LOS channel accounting for path loss $\mathbf{H}_{\text{LOS}}$ are given by

$$\left[\overline{\mathbf{H}}_{\text{LOS}}\right]_{m,n} = \exp\left(\frac{-j2\pi\|\mathbf{p}_n - \mathbf{q}_m\|}{\lambda}\right) \tag{2}$$

$$\left[\mathbf{H}_{\text{LOS}}\right]_{m,n} = \frac{\lambda}{4\pi\|\mathbf{p}_n - \mathbf{q}_m\|}\left[\overline{\mathbf{H}}_{\text{LOS}}\right]_{m,n} \tag{3}$$

where λ is the wavelength and $\|\mathbf{p}_n - \mathbf{q}_m\|$ is the distance between the n-th UAV and the m-th GS antenna. The element of the m-th row, n-th column of a matrix $\mathbf{X}$ is denoted by $[\mathbf{X}]_{m,n}$. The n-th UAV is located at position $\mathbf{p}_n \in \mathbb{R}^3$ defined as $\mathbf{p}_n = [x_n, y_n, z_n]$. Similarly, the m-th ground antenna is located at position $\mathbf{q}_m \in \mathbb{R}^3$. The matrix $\mathbf{P} \in \mathbb{R}^{3\times N}$ contains all the UAV positions such that $\mathbf{P} = [\mathbf{p}_0^T, \cdots, \mathbf{p}_{N-1}^T]^T$ with $()^T$ denoting the transpose.

The GS is assumed to be arranged as a $M_x \times M_z$ uniform rectangular array where $M = M_x \times M_z$. Without loss of generality, the GS is assumed to be placed in the x-z plane with $\mathbf{q}_0 = [0, 0, 0]^T$ used as a coordinate reference. The spacing between the antennas in the x and z directions is given by d_x and d_z respectively. Hence, $\mathbf{q}_m = [i_m d_x, 0, j_m d_z]^T$, where i_m and j_m are the antennas indices in x and z directions respectively and satisfy $m = i_m M_z + j_m$. The average separation along the y-axis between the UAVs and the GS is given by $R = \frac{\sum_{n=0}^{N-1} y_n}{N}$. The system model is illustrated in Fig. 1.

We assume that the UAV swarm operates within a bounded region in the far-field and that the GS is pointed toward the swarm such that $\mathbf{P} \in \mathcal{F}$ where $\mathcal{F}$ is a position set defined as

$$\mathcal{F} = \Big\{\mathbf{P} \mid y_n \gg |y_n - y_m|,\ y_n \gg |x_n|,\ y_n \gg |z_n|,\ y_n \gg M_x d_x,\ y_n \gg M_z d_z,\ n, m \in \{0, \cdots, N-1\}\Big\} \tag{4}$$

In this work, the swarm is always assumed to be within the set $\mathcal{F}$. Using these assumptions, the magnitude of all the elements of the LOS channel matrix can be approximated to be constant and equal to $\frac{\lambda}{4\pi R}$ such that

$$\mathbf{H}_{\text{LOS}} \approx \frac{\lambda}{4\pi R}\overline{\mathbf{H}}_{\text{LOS}} \tag{5}$$

The single user bound defines the maximum achievable capacity and is given by [37]

$$C = \log\det\left(\mathbf{I} + \rho\mathbf{H}^H\mathbf{H}\right) \leq \sum_{n=0}^{N-1}\log\left(1 + \rho\|\mathbf{h}_n^{[c]}\|^2\right) = C_{\max} \tag{6}$$

Authorized licensed use limited to: ASU Library. Downloaded on August 18,2023 at 20:13:23 UTC from IEEE Xplore. Restrictions apply.

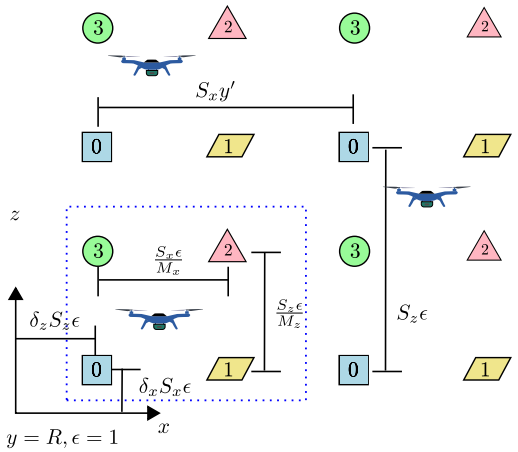

Fig. 2. An illustration of the set $\mathcal{P}$ for a swarm placed on the same plane at $y = R$ for a 2×2 URA. The numbered colored shapes identify different positions. Each UAV needs to occupy a different position to maximize capacity.

where ρ is the signal to noise ratio and $\mathbf{h}_n^{[c]}$ is the n-th column of $\mathbf{H}$ and $()^H$ denote the Hermitian transpose. The maximum capacity given by the single user bound $C_{\max}$ can be attained when the columns of the channel matrix are mutually orthogonal [37]. When the bound is reached, the N different data streams do not interfere with each other. Using the magnitude approximation, the channel maximizing the capacity has to realize

$$\mathbb{E}\{\mathbf{H}^H\mathbf{H}\} = M\left(\frac{\lambda}{4\pi R}\right)^2 \mathbf{I} \tag{7}$$

where $\mathbf{I}$ is the $N \times N$ identity matrix and $\mathbb{E}\{\}$ denotes the expectation with respect to the channel NLOS component. Equation (7) defines the condition on the channel matrix to attain the single-user bound capacity $C_{\max}$. However, to formulate an optimization problem over the UAV positions, we need to relate the UAV positions with (7). Our objective is to define a set of UAV positions that realize equation (7) in order to maximize the capacity. Later, this set is used in the problem formulation.

IV. Set of Capacity Maximizing Positions

For an M antenna GS, the maximum number of UAVs capable of using spatial multiplexing is M. In this section, we aim to define the M positions for these UAVs that maximize the capacity. If the number of UAVs, N, is less than M, the UAVs can be placed to occupy only N of these M positions. So without loss of generality, we consider the matrix $\mathbf{H}$ to be a square matrix of size $M \times M$ and (7) can be rewritten in terms of the rows (instead of the columns) of $\mathbf{H}$ as

$$\mathbb{E}\{\mathbf{h}_l^H\mathbf{h}_k\} = \begin{cases} M\left(\frac{\lambda}{4\pi R}\right)^2 & l = k \\ 0 & l \neq k \end{cases} \tag{8}$$

where $\mathbf{h}_k$ is the k-th column of the transposed channel $\mathbf{H}^T$.

Since $\mathbf{H}$ is a Rician channel, due to the NLOS component $\mathbf{H}_{\text{NLOS}}$, its elements are random variables. In our derivations, we consider the expected value of the columns inner product given by $\mathbb{E}\{\mathbf{h}_l^H\mathbf{h}_k\}$. Given our assumption that the elements $\mathbf{H}_{\text{NLOS}}$ are independent and zero mean, $\mathbb{E}\{\mathbf{h}_l^H\mathbf{h}_k\} = \mathbf{h}_l^{H[\text{LOS}]}\mathbf{h}_k^{[\text{LOS}]}$ for $l \neq k$ where $\mathbf{h}_k^{[\text{LOS}]}$ is the k-th column of $\mathbf{H}_{\text{LOS}}^T$. Hence, using the LOS component in our derivations is equivalent to using the average over the Rician channel. To simplify the notations, we drop the expectation operator and we consider the channel matrix to be normalized such that $\mathbf{H} = \overline{\mathbf{H}}_{\text{LOS}}$.

We start by relating the right-hand side of (8) to the UAV positions as follows

$$\mathbf{h}_l^H\mathbf{h}_k = \sum_{n=0}^{N-1} \exp\left(\frac{-j2\pi}{\lambda}(\|\mathbf{p}_n - \mathbf{q}_l\| - \|\mathbf{p}_n - \mathbf{q}_k\|)\right) \tag{9}$$

To simplify the exponent of (9), we use our far-field assumption to approximate the distance

$$\begin{aligned}\|\mathbf{p}_n - \mathbf{q}_l\| &= \sqrt{(x_n - i_l d_x)^2 + (y_n)^2 + (z_n - j_l d_z)^2} \\ &\approx y_n\left(1 + \frac{1}{2}\left(\frac{x_n - i_l d_x}{y_n}\right) + \frac{1}{2}\left(\frac{z_n - j_l d_z}{y_n}\right)\right)\end{aligned} \tag{10}$$

where i_l and j_l are the antenna indices along x and z respectively and both satisfy $l = i_l M_z + j_l$. The approximation uses the first-order Taylor approximation of the square root assuming that the UAVs are within $\mathcal{F}$. Hence, we can rewrite

$$\mathbf{h}_l^H\mathbf{h}_k \approx \sum_{n=0}^{N-1} \exp\left(\frac{-j2\pi}{y_n\lambda}((-i_l+i_k)d_x x_n + (-j_l+j_k)d_z z_n)\right) \tag{11}$$

Note that from this result, we can see that the rate of change of the phase with respect to x_n and z_n is proportional to $1/y_n$, while the rate of change with respect to y_n is proportional to $1/y_n^2$. Hence, to incur a given phase difference by moving the UAV in the y-direction requires a much larger motion than by moving in the x or z directions. This observation will be used later when optimizing the UAV positions.

We start by describing one value of swarm positions $\mathbf{P}$ that make the channel orthogonal in Lemma 1. After determining these positions, we investigate the changes in positions that retain orthogonality in Lemmas 2 and 3. The set of positions maximizing capacity is obtained by combining these Lemmas in Theorem 1.

Lemma 1: A uniform rectangular arrangement of UAVs within $\mathcal{F}$ having positions given by $x_n = i_n\frac{\lambda y_n}{M_x d_x}$ in the x-direction and $z_n = j_n\frac{\lambda y_n}{M_z d_z}$ in the z-direction realize channel orthogonality, where $i_n \in \{0, \cdots, M_x - 1\}$ and $j_n \in \{0, \cdots, M_z - 1\}$ such $n = i_n M_z + j_n$.

Proof: See Appendix A. ■

Lemma 1 determines one value of swarm positions $\mathbf{P}$, which makes the channel orthogonal. Now, we consider a few changes to positions that do not affect orthogonality.

Lemma 2: Shifting the UAV swarm in the x-z plane such that each UAV is shifted proportionally to its y separation from

Authorized licensed use limited to: ASU Library. Downloaded on August 18,2023 at 20:13:23 UTC from IEEE Xplore. Restrictions apply.

the GS does not affect channel orthogonality as long as the swarm remains within $\mathcal{F}$.

Proof: Let the set of UAV positions $\mathbf{P}$ realize $\mathbf{h}_l^H \mathbf{h}_k = 0$ for all $l \neq k$. Let $\mathbf{h}'_l$ and $\mathbf{h}'_k$ be columns of the channel after shifting UAV n by $\delta_x y_n$ for all n in the x-direction and $\delta_z y_n$ in the z-direction.

$$\begin{aligned}\mathbf{h}_l^{'H}\mathbf{h}'_k &= \sum_{n=0}^{N-1} \exp\left(\frac{-j2\pi}{y_n\lambda}\left((-i_l+i_k)d_x\left(x_n+\delta_x y_n\right)\right.\right.\\ &\quad \left.\left.+(-j_l+j_k)d_z\left(z_n+\delta_z y_n\right)\right)\right)\\ &= \exp\left(\frac{-j2\pi}{\lambda}((-i_l+i_k)\delta_x+(-j_l+j_k)\delta_z)\right)\mathbf{h}_l^H\mathbf{h}_k\\ &= 0 \end{aligned} \tag{12}$$

Hence, UAV shifts scaled with respect to their y coordinate do not affect the orthogonality of the MIMO channel. ■

Lemma 3: Translation of individual UAVs such that UAV n is translated by an integer multiple of $\frac{\lambda y_n}{d_x}$ in x-direction and/or $\frac{\lambda y_n}{d_z}$ in z-direction does not affect the channel orthogonality as long as the swarm remains within $\mathcal{F}$.

Proof: Let the channel have columns $\mathbf{h}_l$ and $\mathbf{h}_k$ for some GS antennas l and k. Let all UAVs be translated independent of each other, such that UAV n is shifted by $f_n\frac{\lambda y_n}{d_x}$ and $g_n\frac{\lambda y_n}{d_z}$ in the x and z-direction respectively for some UAV specific integers f_n and g_n. Let $\mathbf{h}'_l$ and $\mathbf{h}'_k$ be columns of the channel after the shifting. Calculating the inner product of these columns, we get

$$\begin{aligned}\mathbf{h}_l^{'H}\mathbf{h}'_k &= \sum_{n=0}^{N-1} \exp\left(\frac{-j2\pi}{y_n\lambda}\left((-i_l+i_k)d_x\left(x_n+f_n\frac{\lambda y_n}{d_x}\right)\right.\right.\\ &\quad \left.\left.+(-j_l+j_k)d_z\left(z_n+g_n\frac{\lambda y_n}{d_z}\right)\right)\right)\\ &= \exp\left(-j2\pi((-i_l+i_k)f_n+(-j_l+j_k)g_n)\right)\mathbf{h}_l^H\mathbf{h}_k\\ &= \mathbf{h}_l^H\mathbf{h}_k \end{aligned} \tag{13}$$

■

In addition to scaled swarm translations from Lemmas 2 and individual UAV jumps from Lemma 3, it easy to see that permuting the positions of the swarm does not affect orthogonality. We define a set of positions orthogonalizing the channel by combining the three previous lemmas as follows.

Theorem 1: Given a URA GS with M antennas, the set $\mathcal{P} \subset \mathcal{F}$ is a set containing placements, $\mathbf{P} \in \mathbb{R}^{3\times M}$, of M UAVs, which realize the channel orthogonality condition given by (8). The set $\mathcal{P}$ can be described given the environment constants $S_x = \frac{\lambda R}{d_x}$ and $S_z = \frac{\lambda R}{d_z}$ as follows

$$\begin{aligned}\mathcal{P} = \{&\mathbf{P} : \mathbf{P} = \mathbf{T}_\Pi\widetilde{\mathbf{P}},\ \widetilde{\mathbf{P}} \in \mathcal{F},\\ &x_n = \left[\widetilde{\mathbf{P}}\right]_{0,n}, \epsilon_n = \frac{\left[\widetilde{\mathbf{P}}\right]_{1,n}}{R}, z_n = \left[\widetilde{\mathbf{P}}\right]_{2,n}\\ &x_n = i_n\frac{S_x\epsilon_n}{M_x} + f_nS_x\epsilon_n + \delta_xS_x\epsilon_n,\\ &z_n = j_n\frac{S_z\epsilon_n}{M_z} + g_nS_z\epsilon_n + \delta_zS_z\epsilon_n\, n = i_nM_z + j_n,\\ &\quad i_n \in \{0,\cdots,M_x-1\}, j_n \in \{0,\cdots,M_z-1\},\\ &\quad \mathbf{T}_\Pi \in \Pi^M, \delta_x, \delta_z \in \mathbb{R}, f_n, g_n \in \mathbb{Z}\forall n\} \end{aligned} \tag{14}$$

where Π^M is the set of all $M \times M$ permutation matrices.

Proof: This can be proved by the application of Lemmas 2, 3, and applying permutations on the results obtained by Lemma 1. We renamed $y_n = \epsilon_n R$ and the shifts from Lemma 2 to $\delta_x S_x \epsilon_n$ and $\delta_z S_z \epsilon_n$ for convenience of notation. ■

If the swarm positions are within $\mathcal{P}$ as defined in Theorem 1, the orthogonality condition (7) is satisfied and $C_{\max}$ is attained. By using this set, an optimization problem over UAV positions can be formulated. We show an example of the set $\mathcal{P}$ in Fig. 2 for a simple scenario having $M = 4$ with $M_x = M_z = 2$ and $N = 3$ UAVs on the same x-z plane. The positions defined according to Lemma 1 are labeled 0 to 3 in different colored shapes inside the blue dotted square. According to Lemma 3, The $S_x\epsilon$ and the $S_z\epsilon$ jumps along x and z respectively are also within $\mathcal{P}$. This entire grid can be shifted by δ_x and δ_z according to Lemma 2. Orthogonality is attained by assigning the 3 UAVs to any of the 4 positions. After defining the set of UAV positions, $\mathcal{P}$, orthogonalizing the channel and attaining $C_{\max}$, we discuss the problem formulation.

V. Placement Optimization Problem Formulation

There are several ways to mathematically formulate the problem of optimizing swarm positions to attain the maximum capacity. The most intuitive way is to optimize over the positions with the capacity as the objective. However, since any swarm positions $\mathbf{P} \in \mathcal{P}$ can achieve $C_{\max}$ and no unique solution exists, using this formulation, the obtained positions can be far from the UAVs' initial positions and hence would cause unnecessary disturbance to the deployment application. Given that the considered deployment application prioritizes communications with no hard constraints on UAV displacement, defining a constraint on the distance traveled by the UAVs is not straightforward; if the constraint is too tight, a suboptimal capacity below $C_{\max}$ will be achieved, if the constraint is too loose, the solution might lead to unnecessary travel by the UAVs. The minimal distance to attain $C_{\max}$ differs from one deployment environment to the other and hence cannot be used as a constraint. Instead, we make minimizing the distance traveled our objective. To guarantee that the maximum capacity is attained, we constrain the optimized UAV positions to be within the set $\mathcal{P}$, which attains $C_{\max}$. This formulation attains the maximum capacity with the least traveled distance.

A mathematical formulation of the problem is as follows; Given N UAVs with initial positions $\{\overline{\mathbf{p}}_0, \overline{\mathbf{p}}_1, \cdots, \overline{\mathbf{p}}_{N-1}\}$, where $\overline{\mathbf{p}}_n = [\overline{x}_n, \overline{y}_n, \overline{z}_n]^T$. These initial positions are assumed to be determined by the deployment application. Our objective is to find the nearest UAV positions which belong to $\mathcal{P}$. This problem can be formulated as

$$\begin{aligned}&\underset{\{\mathbf{p}_m\},\{b_{m,n}\}}{\text{minimize}} \sum_{m=1}^{M}\sum_{n=1}^{N} b_{m,n}\|\overline{\mathbf{p}}_n - \mathbf{p}_m\|\\ &\text{subject to } [\mathbf{p}_0,\cdots,\mathbf{p}_{M-1}] \in \mathcal{P}\\ &\qquad \sum_{n=0}^{N} b_{m,n} \leq 1 \quad \forall m, \quad \sum_{m=0}^{M} b_{m,n} = 1 \quad \forall n\\ &\qquad b_{m,n} \in \{0,1\} \quad \forall m,n \end{aligned} \tag{15}$$

Authorized licensed use limited to: ASU Library. Downloaded on August 18,2023 at 20:13:23 UTC from IEEE Xplore. Restrictions apply.

The binary variable $b_{m,n}$ is used to assign each of the N UAVs (indexed using n) to one of the M positions within $\mathcal{P}$ (indexed using m). This problem formulation does not make any assumptions about whether the UAVs are transmitters or receivers and does not make any assumptions about the transmitter and receiver processing. Later in Section VIII, we consider an uplink scenario and derive the optimal linear precoders and combiners.

Using the definition of $\mathcal{P}$ from Theorem 1 in (15), the problem can be rewritten as

$$\begin{aligned}
&\underset{\substack{\{x_m\},\{y_m\},\{z_m\},\\ \delta_x,\delta_z,\{\epsilon_n\},\\ \{f_m\},\{g_m\},\{b_{m,n}\}}}{\text{minimize}} \quad \sum_{m=0}^{M-1}\sum_{n=0}^{N-1} b_{m,n}\sqrt{(x_m-\overline{x}_n)^2+(y_m-\overline{y}_n)^2+(z_m-\overline{z}_n)^2} \\
&\text{subject to } x_m = i_m\frac{S_x\epsilon_m}{M_x} + f_m S_x\epsilon_m + \delta_x S_x\epsilon_m, \quad \forall m \\
&\qquad z_m = j_m\frac{S_z\epsilon_m}{M_z} + g_m S_z\epsilon_m + \delta_z S_z\epsilon_m, \quad \forall m \\
&\qquad f_n, g_n \in \mathbb{Z} \quad \forall n \\
&\qquad \sum_{n=0}^{N} b_{m,n} \le 1 \quad \forall m, \quad \sum_{m=0}^{M} b_{m,n} = 1 \quad \forall n \\
&\qquad b_{m,n} \in \{0,1\} \quad \forall m,n \\
&\qquad -\frac{1}{2} \le \delta_x \le \frac{1}{2}, -\frac{1}{2} \le \delta_z \le \frac{1}{2} \\
&\qquad y_m = R\epsilon_m
\end{aligned} \tag{16}$$

where $i_m \in \{0,\cdots,M_x\}$ and $j_m \in \{0,\cdots,M_z\}$ and both satisfy $m = i_m M_z + j_m$. In the current form, this problem is a non-convex mixed-integer problem that is not tractable.

To solve this problem, we consider both an offline centralized solution in Section VI and an online distributed algorithm in Section VII. The centralized solution assumes the initial positions are known apriori and aims to relax and solve (16). In the case where the UAVs are already deployed without prior knowledge of their placements, a distributed online algorithm where the UAVs iteratively improve their positions is also proposed.

VI. Centralized Offline Solution

For the centralized solution, we start by relaxing problem (16) to make it more tractable prior to deriving its solution. An upper bound for the distance traveled and the time complexity are also discussed.

A. Problem Relaxation

We start by eliminating the y-translation variable.

1) Eliminating y-Translation: As discussed previously y_m has a small effect on the phase unlike a change in x_m and z_m. A UAV has to travel a much larger distance along the y direction compared to the x or z direction to incur a phase change. So to simplify, we relax the problem by not optimizing over the y-translation, i.e, setting $y_m = \overline{y}_m$ for all UAVs. Hence, we only optimize over x_m and z_m. Given this simplification, the y term in the objective is equal to zero and ϵ_m becomes a constant for all m. The problem can be reformulated as

$$\underset{\substack{\{x'_{m,n}\},\{z'_{m,n}\},\\ \{f_n\},\{g_n\}\\ \{b_{m,n}\}\\ \delta_x,\delta_z}}{\text{minimize}} \sum_{m=0}^{M-1}\sum_{n=0}^{N-1} b_{m,n}\sqrt{(x'_{m,n})^2+(z'_{m,n})^2} \tag{17}$$

$$\text{subject to } x'_{m,n} = i_m\frac{S_x\epsilon_n}{M_x} + f_m S_x\epsilon_n + \delta_x S_x\epsilon_n - \overline{x}_n, \forall n,m \tag{18}$$

$$z'_{m,n} = j_m\frac{S_z\epsilon_n}{M_z} + g_m S_z\epsilon_n + \delta_z S_x\epsilon_n - \overline{z}_n, \forall n,m \tag{19}$$

$$f_n, g_n \in \mathbb{Z} \quad \forall n \tag{20}$$

$$b_{m,n} \in \{0,1\} \quad \forall n,m \tag{21}$$

$$\sum_{n=0}^{N} b_{m,n} \le 1 \ \ \forall m, \quad \sum_{m=0}^{M} b_{m,n} = 1 \quad \forall n \tag{22}$$

$$-\frac{1}{2} \le \delta_x \le \frac{1}{2}, \quad -\frac{1}{2} \le \delta_z \le \frac{1}{2} \tag{23}$$

The value of $x'_{m,n}$ is the x-translation difference between the initial position of UAV n and the optimal position m and $z'_{m,n}$ is similarly defined for the z-translation. The integers f_m and g_m define multiple possible solutions, however, we know that the optimal one is closer to the starting positions. We use this intuition to narrow the solution space.

2) Narrowing Solution Space: According to Lemma 3, any integer value of f_m and g_m can achieve orthogonality. However, the values of these variables that minimize the translation are expected to be the ones closest to the starting positions of the UAVs. To simplify the problem using this intuition, we start by rewriting the initial positions of the UAVs $\overline{x}_n$ and $\overline{z}_n$ as a function of our environment constants as follows $\overline{x}_n = c'_n S_x\epsilon_n$ where c'_n is the constant satisfying this relation. By substituting in (18), we get

$$\begin{aligned}
\frac{i_m}{M_x}S_x\epsilon_n + f_m S_x\epsilon_n - \overline{x}_n &= S_x\epsilon_n\left(f_m + \frac{i_m}{M_x} - c'_n\right) \\
&= S_x\epsilon_n\left(f_m - (f'_n + r'_n)\right) \\
&= \tilde{x}_{m,n} + f_{m,n}S_x\epsilon_n
\end{aligned} \tag{24}$$

where $f'_n = \left\lfloor \frac{i_m}{M_x} - c'_n \right\rfloor$ is an integer obtained by the floor operation and $r'_n = \left(\frac{i_m}{M_x} - c'_n\right) - f'_n$ has a magnitude smaller than one. The distance $\tilde{x}_{m,n}$ is defined as $\tilde{x}_{m,n} = S_x\epsilon_n r'_n$ and satisfies $0 \le \tilde{x}_n < S_x\epsilon_n$. We define $f_{m,n} = f_m - f'_n$, which redefines the integer translations to use the initial positions of the UAV n as a starting point. Hence, we can rewrite (18) as

$$x'_{m,n} = \tilde{x}_{m,n} + f_{m,n}S_x\epsilon_n + \delta_x S_x\epsilon_n \tag{25}$$

similarly for the z-direction, we get

$$z'_{m,n} = \tilde{z}_{m,n} + g_{m,n}S_z\epsilon_n + \delta_z S_z\epsilon_n \tag{26}$$

Proposition 1: The value of $f_{m,n}$ and $g_{m,n}$ that minimizes (17) is within the set $\{-1,0\}$ and is given by

$$\hat{f}_{m,n} = \begin{cases} 0 & -\frac{1}{2}S_x\epsilon_n \le \tilde{x}_{m,n} + \delta_x S_x\epsilon_n < \frac{1}{2}S_x\epsilon_n \\ -1 & \frac{1}{2}S_x\epsilon_n \le \tilde{x}_{m,n} + \delta_x S_x\epsilon_n \le \frac{3}{2}S_x\epsilon_n \end{cases} \tag{27}$$

Authorized licensed use limited to: ASU Library. Downloaded on August 18,2023 at 20:13:23 UTC from IEEE Xplore. Restrictions apply.

Proof: See Appendix B. ∎

A similar result can be proved for $g_{m,n}$. Hence, among all the values of integer translations from the initial UAV positions, $f_{m,n}$ and $g_{m,n}$, we only need to consider the values of the nearest translations from the UAV's initial locations.

3) The Relaxed Problem: The problem is thus simplified to

$$\begin{aligned}
&\underset{\substack{\{x'_n\},\{z'_n\},\\ \{f_{m,n}\},\{g_{m,n}\}\\ \{b_{m,n}\}\\ \delta_x,\delta_z}}{\text{minimize}} \sum_{m=0}^{M-1}\sum_{n=0}^{N-1} b_{m,n}\sqrt{(x'_{m,n})^2+(z'_{m,n})^2}\\
&\text{subject to } x'_{m,n} = \tilde{x}_{m,n} + f_{m,n}S_x\epsilon_n + \delta_x S_x\epsilon_n, \quad \forall n,m\\
&\qquad z'_{m,n} = \tilde{z}_{m,n} + g_{m,n}S_z\epsilon_n + \delta_z S_z\epsilon_n, \quad \forall n,m\\
&\qquad f_{m,n}, g_{m,n} \in \{-1,0\} \quad \forall n\\
&\qquad b_{m,n} \in \{0,1\} \quad \forall n,m\\
&\qquad \sum_{n=0}^{N} b_{m,n} \le 1 \quad \forall m, \quad \sum_{m=0}^{M} b_{m,n} = 1 \quad \forall n\\
&\qquad -\frac{1}{2} \le \delta_x \le \frac{1}{2}, \quad -\frac{1}{2} \le \delta_z \le \frac{1}{2} \qquad (28)
\end{aligned}$$

B. Problem Solution

The problem (28) still remains a non-convex mixed-integer problem. The difficulty in solving the problem is because the variables δ_x and δ_z are common to the entire swarm. We show that by for a given value of some variables the problem becomes tractable and we use that fact to solve the problem.

1) Solution Given δ_x and δ_z: For a given value of δ_x and δ_z, the problem becomes tractable and it can be solved as follows: first, we minimize over $f_{m,n}$ and $g_{m,n}$ using (27) since δ_x and δ_z are given. Once these values have been calculated, the square root term in the objective becomes a constant. What remains is to solve for $b_{m,n}$, which becomes the following integer linear program

$$\begin{aligned}
&\underset{\{b_{m,n}\}}{\text{minimize}} \sum_{m=0}^{M-1}\sum_{n=0}^{N-1} b_{m,n}\sqrt{(x'_{m,n})^2+(z'_{m,n})^2}\\
&\text{subject to } b_{m,n} \in \{0,1\} \quad \forall n,m\\
&\qquad \sum_{n=0}^{N} b_{m,n} = 1 \quad \forall m, \quad \sum_{m=0}^{M} b_{m,n} \le 1 \quad \forall n \qquad (29)
\end{aligned}$$

This integer program can be shown to be equivalent to its real relaxation. This problem is indeed an assignment problem that can be solved in polynomial time using the Hungarian algorithm [38].

2) Solution Given an Assignment: Again considering (28), the challenge in solving for δ_x and δ_z is that they are multiplied by integer variables $b_{m,n}$. Given an assignment defining the values of $b_{m,n}$, the problem (28) becomes the following convex problem

$$\begin{aligned}
&\underset{\substack{\{x'_n\},\{z'_n\},\\ \delta_x,\delta_z}}{\text{minimize}} \sum_{m=0}^{M-1}\sum_{n=0}^{N-1} b_{m,n}\sqrt{(x'_{m,n})^2+(z'_{m,n})^2}\\
&\text{subject to } x'_{m,n} = \tilde{x}_{m,n} + \hat{f}_{m,n}S_x\epsilon_n + \delta_x S_x\epsilon_n, \quad \forall n,m\\
&\qquad z'_{m,n} = \tilde{z}_{m,n} + \hat{g}_{m,n}S_z\epsilon_n + \delta_z S_z\epsilon_n, \quad \forall n,m\\
&\qquad -\frac{1}{2} \le \delta_x \le \frac{1}{2}, \quad -\frac{1}{2} \le \delta_z \le \frac{1}{2} \qquad (30)
\end{aligned}$$

which can be solved using a convex solver like CVXPY [39].

3) Complete Solution: We have shown that for a given δ_x and δ_z, (28) gets simplified to (29) which can be optimally solved. We also have shown that for a given $b_{m,n}$, we get (30) which can also be optimally solved. Hence, to solve (28), we use block coordinate descent. We optimize over each set of variables in an alternating manner, until the solution stops changing. Since both (29) and (30) are solved to optimality, Problem (28) is guaranteed to converge to a stationary point [40, Prop. 2.7.1]. After solving, we obtain the optimal $\hat{\delta}_x$, $\hat{\delta}_z$, and $\hat{b}_{m,n}$ for all m and n, along with $\hat{f}_{m,n}$ and $\hat{g}_{m,n}$. We need to substitute back to get the UAV positions. From $\hat{b}_{m,n}$, the index of the placement assigned to the n-th UAV $\hat{m}_n$ is given by $\hat{m}_n = \underset{m}{\text{argmax}}\hat{b}_{m,n}$. The assigned position is then calculated using

$$x_n = \tilde{x}_{\hat{m}_n,n} + \hat{f}_{\hat{m}_n,n}S_x\epsilon_n + \hat{\delta}_x S_x\epsilon_n + \overline{x}_n \qquad (31)$$

similarly for the z position

$$z_n = \tilde{z}_{\hat{m}_n,n} + \hat{g}_{\hat{m}_n,n}S_z\epsilon_n + \hat{\delta}_z S_z\epsilon_n + \overline{z}_n \qquad (32)$$

The centralized solution algorithm is summarized in Algorithm 1. Hence, using block coordinate descent, we obtained a suboptimal solution of (28), which is a relaxation of (15).

C. Upper Bound and Time Complexity

The upper bound for the translation of UAVs is derived in Proposition 2

Proposition 2: The maximum absolute translation of UAV n is upper bounded by $\frac{\sqrt{S_x^2+S_z^2}}{2}\epsilon_n$.

Proof: See Appendix C. ∎

As for the algorithm computational complexity, it is the sum of the solution complexities of solving (29) and (30) times the number of iterations. For the number of iterations, convergence typically occurred within fewer than five iterations, which can be enforced as a maximum number of iterations. The Hungarian algorithm used to solve (29) has complexity $\mathcal{O}(M^3)$ [41]. For problem (30), CVXPY [39] uses ECOS second-order cone programming solver [42], which relies on an interior-point algorithm based on Mehrorta predictor-corrector method. In general, the interior points algorithms' complexity depends on the number of variables [43]. Since problem (30) has only two variables (δ_x and δ_z) regardless of the problem size, the solution time is dominated by the Hungarian algorithm. By limiting the iterations to five, the complexity of Algorithm 1 is approximately $\mathcal{O}(M^3)$.

VII. Distributed Online Solution

In the case where the UAV positions are not known before deployment, we develop an iterative distributed approach to be applied within the swarm in realtime. This approach uses channel estimates instead of positions for optimization and it attempts to minimize the inter-swarm communication overhead. In this approach, the UAVs agree on a formation, in which each UAV designates another UAV as its neighbor

Authorized licensed use limited to: ASU Library. Downloaded on August 18,2023 at 20:13:23 UTC from IEEE Xplore. Restrictions apply.

Algorithm 1: Centralized Solution

input : The initial positions of the UAV swarm $\{\overline{\mathbf{p}}_0, \overline{\mathbf{p}}_1, \cdots, \overline{\mathbf{p}}_{N-1}\}$, The parameters of the GS M_x, M_z, d_x, d_z. The wavelength λ.
output: The optimized UAV positions.
current_obj $= \infty$;
previous_obj $= 0$;
Initialize $\delta_x = 0$ and $\delta_z = 0$;
while current_obj-previous_obj>1e-5 **do**
  previous_obj $=$ current_obj ;
  Solve (29) for $\{b_{m,n}\}$ using δ_x and δ_z;
  Solve (30) for δ_x and δ_z using $\{b_{m,n}\}$ and assign the objective value to current_obj ;
end
Calculate the position of UAVs, using (31) and (32)

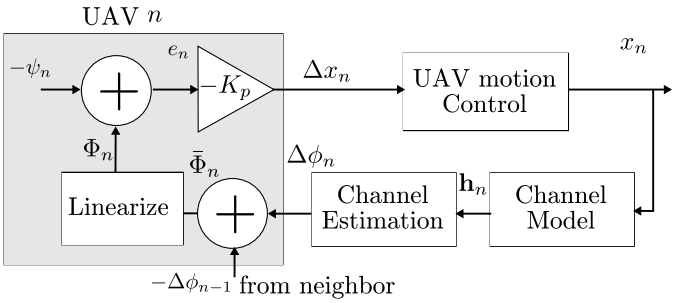

Fig. 3. The closed loop feedback system in UAV n where $n \in \{1, \cdots, N-1\}$. The calculations made on the UAV are highlighted in gray. The value $\Delta\phi_{n-1}$ is obtained from the previous neighbor.

along each axis according to a criterion discussed later. For a ULA GS, this formation is linear, and for a URA it is a rectangular grid. Each UAV estimates its channel and shares the estimates with its neighbors using an ideal control side channel. Using the neighbor channel measurements, the UAVs calculate an error signal. This error signal drives a closed loop feedback system, which decides the magnitude and direction of its motion. In this approach, each UAV moves based on information from its neighbor, as if each UAV exerts a force on its neighbor. Hence, we refer to this approach as Force Field (FF). We start by deriving the fundamentals of this approach and show its convergence on a ULA GS aligned to the x-axis. Then, we discuss how it is applied to a URA GS. In the end, we discuss how the agreement on the formation is performed.

A. Fundamentals of Force Field

The key idea behind FF is that for any optimal positions $\mathbf{P} \in \mathcal{P}$, the equivalent $M \times M$ channel matrix $\mathbf{H}$ can be shown to be a scaled and permuted DFT matrix [44]. The phase difference between successive elements of the l-th column of the DFT matrix is $\frac{2\pi}{M}$. Hence, the phase difference at UAV n due to two consecutive ground antennas l and $l+1$ is given by

$$\Delta\phi_n = \phi_{l,n} - \phi_{l+1,n} = 2\pi f'_n + n\left(\frac{2\pi}{M_x}\right). \tag{33}$$

where $\phi_{l,n} = \angle[\mathbf{H}]_{l,n}$ is the phase of the channel between GS antenna l and UAV n for some integer f'_n. If (33) is satisfied for all UAVs $n \in \{0, \cdots N-1\}$, and all GS antennas $l \in \{0, \cdots M-2\}$, the channel $\mathbf{H}$ is an orthogonal scaled DFT matrix and the capacity is maximized. However, (33) determines the position of each UAV solely on its index n regardless of the remaining UAVs. This might lead to larger distance traveled since each UAV does not consider its neighbors' positions or channels. Additionally, if a UAV suffered from an external disturbance like wind, the remaining UAVs will not adapt. To make each UAV adapt to its neighbors, we reformulate (33) to

$$\Delta\phi_n - \Delta\phi_{n-1} = 2\pi f_n + \left(\frac{2\pi}{M_x}\right) \tag{34}$$

for any integer f_n. Here we assume that the UAV formation has been established and UAV $n-1$ shares its channel estimates with its neighbor UAV n. If all UAVs realize (34), $\mathbf{H}$ becomes orthogonal. We define the difference between the right and the left sides of (34) as an error signal as follows

$$e_n = \Delta\phi_n - \Delta\phi_{n-1} - \psi_n \tag{35}$$

where $\psi_n = 2\pi f_n + \left(\frac{2\pi}{M_x}\right)$ is the target phase difference for some integer f_n. The objective of each UAV is to move such that this error signal is equal to zero. We define $\overline{\Phi}_n = \Delta\phi_n - \Delta\phi_{n-1}$ as the measured state of our system. When each UAV moves, this state changes and our goal is to make it equal to ψ_n. Using the distance approximation (10) based on the far-field assumption, we get

$$\overline{\Phi}_n = (\Delta\phi_n - \Delta\phi_{n-1})\%(2\pi) \tag{36}$$

$$\approx \left(2\pi\left(\frac{x_n}{\epsilon_n} - \frac{x_{n-1}}{\epsilon_{n-1}}\right)\frac{1}{S_x}\right)\%(2\pi) \tag{37}$$

where the environment constant $S_x = \frac{\lambda R}{d_x}$ (as previously defined) and $\%$ denotes the modulus operator. The modulus operation accounts for phase wraps. This relation would have been linear if it was not for the phase ambiguity. Using phase measurements only, we cannot tell whether the UAV did not change position or moved to create a 2π phase difference. However, this ambiguity can be mitigated and the phase unwrapped by limiting the translation that each UAV performs at each step as discussed later. After unwrapping the phase, the system becomes a linear system. Based on the error signal, each UAV can change its position to orthogonalize the channel using a closed loop feedback system.

B. Force Field Algorithm

The proposed feedback system is run iteratively in all UAVs. In iteration k, all the UAVs move simultaneously, except the first UAV which is used as an anchor and does not move. This approach is described as follows: Each UAV estimates its channel and calculates $\Delta\phi_n[k]$ at iteration k. It shares this value with its direct neighbor in the formation, so that UAV n knows $\Delta\phi_{n-1}[k]$ from its neighbor. Each UAV calculates the measured state $\overline{\Phi}_n[k]$ and estimates the unwrapped phase

Authorized licensed use limited to: ASU Library. Downloaded on August 18,2023 at 20:13:23 UTC from IEEE Xplore. Restrictions apply.

state Φ_n using

$$\Phi_n[k] = \begin{cases} \overline{\Phi}_n[k] + 2\pi \left\lfloor \dfrac{\Phi_n[k-1]}{2\pi} \right\rfloor & c = 0 \\ \overline{\Phi}_n[k] + 2\pi + 2\pi \left\lfloor \dfrac{\Phi_n[k-1]}{2\pi} \right\rfloor & c = 1 \\ \overline{\Phi}_n[k] - 2\pi + 2\pi \left\lfloor \dfrac{\Phi_n[k-1]}{2\pi} \right\rfloor & c = 2 \end{cases} \quad (38)$$

where

$$c = \text{argmin}\{|\overline{\Phi}_n[k] - \overline{\Phi}[k-1]|, |\overline{\Phi}_n[k] + 2\pi - \overline{\Phi}[k-1]|, |\overline{\Phi}_n[k] - 2\pi - \overline{\Phi}[k-1]|\} \quad (39)$$

It is easy to verify that phase wrap errors will not occur as long the phase transition between iterations is less than π. After linearizing the state, each UAV calculates an error $e_n[k]$ using (35). Based on this error signal, it changes its position such that

$$x_n[k+1] = x_n[k] - K_p e_n^{[x]}[k] \quad (40)$$

where K_p is a constant creating a proportional controller. The first UAV in the formation having $n = 0$ is used as an anchor, i.e, it does not change positions. The closed loop feedback system at UAV n is shown in Fig. 3, with the calculations that run in the UAV highlighted in gray. The input to our approach for UAV n is its phase estimates along with those of UAV $n-1$. The output is the motion given by $\Delta x_n[k] = x_n[k+1] - x_n[k]$. After a predefined time sufficient for calculations in all UAVs, the output $\Delta x_n[k]$ is fed to the UAV motion control system which navigates the UAV. After the swarm settles, these steps can be repeated for a fixed number of iterations until $|\Delta x_n[k]|$ becomes small for all UAVs. Note that since the system was linearized, instead of the proportional controller in (40), more sophisticated controllers like PID can speed up the convergence [45].

We now discuss the convergence of this approach for a single UAV and then generalize to the entire swarm.

Lemma 4: The error in UAV n is guaranteed to converge to zero given that its previous neighbor, UAV $n-1$, is fixed, if $0 < K_p < \frac{\epsilon_n S_x}{4\pi}$.

Proof: See Appendix D. ∎

Theorem 2: The error of all UAVs is guaranteed to converge to zero if $0 < K_p < \frac{\min_n(\epsilon_n) S_x}{4\pi}$.

Proof: UAV 0 acts as an anchor and does not move. Hence, the error of UAV 1, according to Lemma 4 is guaranteed to converge to zero if $0 < K_p < \frac{\epsilon_0 S_x}{4\pi}$. Once, it converges according to Lemma 4 the error of UAV 2 is also guaranteed to converge to zero if $0 < K_p < \frac{\epsilon_1 S_x}{4\pi}$. Similarly, we can show that all N UAVs will converge if $0 < K_p < \frac{\min_n(\epsilon_n) S_x}{4\pi}$. ∎

Note that although the UAVs closer to the fixed UAV converge first, all the non-converged UAVs move simultaneously. As a consequence of simultaneous motion, oscillations might occur; a UAV might move in some direction in an iteration and in the other direction in the following iteration because its previous neighbor has moved. A smaller value of K_p will reduce the magnitude of oscillations.

C. Force Field URA Extension

Next, we discuss the extension from the ULA GS in the x-direction to a URA in the x-z plane. For a URA, each UAV needs to meet the orthogonality criterion (34) in both the x and z directions. The condition along the x-axis is

$$\Delta\phi_n^{[x]} - \Delta\phi_{n-1}^{[x]} = \psi_n^{[x]} \quad (41)$$

where the superscript $[x]$ is to denote x-direction, $\psi_n^{[x]}$ is the x phase objective, and $\Delta\phi_n^{[x]} = \phi_{n,i_m M_z + j_m} - \phi_{n,(i_m+1)M_z + j_m}$ where $i_m M_z + j_m$ and $(i_m+1)M_z + j_m$ are the indices of two consecutive GS antennas along the x-direction. Similar definitions exist for the z-direction using phase calculated for two consecutive GS antennas along the z-direction: $\Delta\phi_n^{[z]} = \phi_{n,i_m M_z + j_m} - \phi_{n,i_m M_z + j_m + 1}$. To realize (41) and its z equivalent, FF is extended to apply the same procedures for a ULA along both directions. Hence, each UAV needs to designate two neighbors, one for each direction. This makes the final FF formation a grid. This grid consists of M_x lines applying linear FF along z direction and M_z lines applying it along the x-direction. The anchor node that does not move in that case is a corner node having both grid indices $i_n = j_n = 0$. We note that for a ULA in the x-direction the set $\mathcal{P}$ is unconstrained in the z-direction. Unlike the ULA, for the URA case, to retain orthogonality over the entire swarm, the UAVs that form a line in the x-direction, need to have the same phase with respect to the z-direction and vice versa. To accomplish that a small modification is made; the first line of the grid in the x-direction (having indices satisfying $n\%M_z = 0$ where $\%$ denotes the modulus operator) applies FF along the z-direction to have a phase difference along z equal to zero. The phase objective along the z direction $\psi_n^{[z]}$ for UAV n in (35) realizing this condition is

$$\psi_n^{[z]} = \begin{cases} 0 & n\%M_z = 0 \\ 2\pi/M_z & \text{otherwise} \end{cases} \quad (42)$$

A similar relation can be derived for the phase objective along x. Since, for a URA, the same FF feedback system is applied along multiple lines with a minor modification, the same convergence proofs apply.

D. Initializing Formations

Last, we describe how the formations are established. As shown in Theorem 2, the convergence only depends on each UAV picking a node as a neighbor along each axis, such that all the UAVs create a grid formation. The method of choosing the neighbor does not affect whether or not convergence will occur, however, it affects the distance that each UAV will travel to orthogonalize the channel. Our proposed approach relies on UAVs creating the formations based on an initial channel estimate that is shared globally among the swarm.

After sharing the channel, all UAVs pick their closest neighbor based on phase relative to the x-direction and then relative to the z direction. Given that the measured phase states along x and z directions are defined as $\overline{\Phi}_N^{[x]} = \Delta\phi_n^{[x]} - \Delta\phi_{n-1}^{[x]}$ and $\overline{\Phi}_N^{[z]} = \Delta\phi_n^{[z]} - \Delta\phi_{n-1}^{[z]}$ respectively. The assignment

Authorized licensed use limited to: ASU Library. Downloaded on August 18,2023 at 20:13:23 UTC from IEEE Xplore. Restrictions apply.

is accomplished in two stages, first, we sort the state along x such that $\overline{\Phi}_0^{[x]} \leq \overline{\Phi}_1^{[x]} \leq \cdots \leq \overline{\Phi}_{N-1}^{[x]}$. Then, each M_z UAVs are divided into a group and sorted such that the m-th group satisfies $\overline{\Phi}_{mM_z}^{[z]} \leq \overline{\Phi}_{mM_z+1}^{[z]} \leq \cdots \leq \overline{\Phi}_{(m+1)M_z-1}^{[z]}$. This assignment guarantees that the phase along any line of UAVs in the grid is increasing.

The entire force field algorithm is summarized in Algorithm 2. The **forall** construct is used to indicate that all UAVs act in parallel. For simplicity, we consider using a fixed number of iterations K_c. More adaptive stopping criteria can easily be developed based on the value of the error or the SINR. Since at convergence the interference among data streams is eliminated, the MIMO SINR is equal to the SNR when a single UAV is communicating with the GS. By setting the target SINR below the SNR, we can sacrifice the achievable capacity in favor of less distance traveled by the UAVs. Next, we find an upper bound for the distance traveled.

Proposition 3: The distance traveled by UAV n when using Force Field is upper bounded by $\left(\sqrt{S_x^2+S_z^2}\right)(\max\{\epsilon_0,\epsilon_n\})$

Proof: For the m-th line in the grid formed by the UAVs along the x direction, UAVs are ordered such that

$$-\pi \leq \overline{\Phi}_m^{[x]} \leq \overline{\Phi}_{M_z+m}^{[x]} \leq \overline{\Phi}_{2M_z+m}^{[x]} \leq \cdots \leq \overline{\Phi}_{(M_x-1)M_z+m}^{[x]} \leq \pi \tag{43}$$

The first UAV is used as an anchor and it does not move. Each UAV is pushing its neighbor to realize a phase difference of $\frac{2\pi}{M_x}$. Since, the formation guarantees that the UAVs are increasing in phase, the worst-case scenario is when all UAVs start at exactly at the same phase. In that case, the UAV having index n will have to travel to create a phase difference of $n\frac{2\pi}{M_x}$ from the start UAV. Using (37), this is equivalent to having $\left(\frac{x_n}{\epsilon_n}-\frac{x_0}{\epsilon_0}\right)=S_x$. From which, $|x_n-x_0| \leq S_x(\max\{\epsilon_0,\epsilon_n\})$. A similar argument can be made for the z-direction. Combining both constraints, we get that the distance traveled by UAV n is upper bounded by $\left(\sqrt{S_x^2+S_z^2}\right)(\max\{\epsilon_0,\epsilon_n\})$. ■

We notice that the traveled distance upper-bound for Force Field is higher than the centralized solution upper-bound from Proposition 2. We also expect that the centralized approach would require less distance traveled than FF for several reasons; First, the centralized approach assumes the knowledge of the UAV initial positions, which define the problem. On the other hand, FF only uses only channel information, from which the positions cannot be recovered. Second, compared to the centralized solution, FF does not optimize the displacement of the entire swarm (from Lemma 2) and just uses the first UAV as an anchor. Having a fixed UAV is crucial to guarantee the convergence as shown in Theorem 2. Third, FF assigns the UAVs to the positions in a simple way based on sorting the phases to avoid running a complicated assignment procedure in all the UAVs.

Algorithm 2: Force Field Algorithm

```
input : M_x, M_z
output: Swarm positioned to maximize capacity.
All UAVs estimates channels and share it ;
forall the UAV n = 0 to N − 1 do
    Sort phase estimates to identify neighbors;
    Calculate phase objective using (42) along x and z;
end
for iterations k = 1 to K_c do
    forall the UAV n = 0 to N − 1 do
        Estimate channel and share with neighbors;
        Calculate state (36) and linearize (38) in x and z;
        Calculate error using (35) along x and z ;
        Wait sufficiently for other UAVs calculations;
        Move in x and z according to (40);
        Wait sufficiently for other UAVs to move;
    end
end
```

E. Time Complexity of Force Field

Since FF is a distributed algorithm, we discuss the complexity from the perspective of one UAV. In the initialization stage, each UAV has $2M$ phase measurements from the entire swarm along x and z directions. Each UAV sorts the phases along x across all UAV and along z as groups of size M_z. Assuming the merge sort algorithm is used, the initialization complexity is given by $\mathcal{O}(M\log M + M_xM_z\log M_z)$. After initialization, each UAV interacts only with one neighbor in the x-direction and one neighbor in the z-direction, regardless of the swarm size making the complexity be a function of only the number of iterations $\mathcal{O}(K_c)$. The fact that beyond initialization FF complexity is independent of the swarm size makes it scalable.

F. Comparison With Existing Distributed Algorithms

We briefly compare FF to Gradient Descent (GD) and Brute Force (BF) which were both proposed in [12]. GD and BF are both iterative algorithms inspired by numerical optimization algorithm; gradient descent, and steepest descent respectively. GD relies on knowledge of the UAV positions and global channel knowledge within the swarm to calculate the gradient of the capacity with respect to positions. In each iteration, in a sequential manner, all UAVs estimate the channel and one UAV moves in the gradient descent direction. BF also relies on global channel knowledge. In a BF iteration, a UAV takes 6 steps in each of the 6 orthogonal directions. For each direction, the channel is estimated and the orthogonality of the channel is evaluated. The UAV retains the position that improved the channel orthogonality. No upper bounds (UB) on distance traveled nor convergence guarantees were derived for BG and GD in [12]. Since GD and BF are based on numerical methods applied to a non-convex objective, it is not easy to analyze their convergence. Unlike BF and GD, in a FF iteration, each UAV only requires knowledge of the channel from its direct neighbors reducing inter-swarm communications overhead. Also, in an FF iteration, all UAVs move simultaneously, thus requiring fewer channel estimates. The comparison between the algorithms is summarized in Table I.

Authorized licensed use limited to: ASU Library. Downloaded on August 18,2023 at 20:13:23 UTC from IEEE Xplore. Restrictions apply.

TABLE I
DISTRIBUTED ALGORITHMS COMPARISON

Aspect	Force Field	Gradient Descent	Brute Force
Channel Estimations	K_c	NK_c	$6NK_c$
Inter-swarm Comm.	Neighbors	Swarm	Swarm
Convergence Proof	Yes	No	No
Distance Upper Bound	Yes	No	No

VIII. Optimizing a Linear Uplink Scenario

So far we discussed algorithms that optimize UAV positions to maximize the channel capacity, which are applicable in the uplink and downlink scenarios regardless of the transmitter and receiver processing. Now, for an uplink scenario with UAVs as transmitters, we consider the joint optimization of the channel $\mathbf{H}$ (through the UAV positions) and the linear precoders $\mathbf{V} \in \mathbb{C}^{N\times N}$ and combiners $\mathbf{W} \in \mathbb{C}^{M\times M}$. We can define the following joint optimization problem

$$\underset{\mathbf{H},\mathbf{W},\mathbf{V}}{\text{maximize}} \left\{ \log\det\left(\mathbf{I} + \frac{1}{N_0 N_f} \left(\mathbf{W}^H\mathbf{H}\mathbf{V}\right)^H \mathbf{W}^H\mathbf{H}\mathbf{V} \right) \right\} \tag{44}$$

where N_0 is the noise power spectral density and N_f is the receiver noise figure, given that $\mathbf{H}$ is a channel matrix defined according to our system model. Each UAV is assumed to be carrying a radio with maximum transmitted power P_T. Since each UAV transmits an independent data stream, $\mathbf{V}$ is constrained to be a diagonal matrix. The columns of the combining matrix $\mathbf{W}$ are assumed to be normalized.

If we define the equivalent channel $\mathbf{H}_{eq} = \mathbf{W}^H\mathbf{H}\mathbf{V}$, according to the upper bound (6), the maximum occurs when $\mathbf{H}_{eq}$ is orthogonal for a given SNR. Maximizing the SNR for an orthogonal $\mathbf{H}_{eq}$ solves (44). Using our proposed position optimization algorithms, the channel $\mathbf{H}$ can be made orthogonal. For orthogonal $\mathbf{H}$, the matched filter combiner given by $\mathbf{W} = \frac{\mathbf{H}}{\|\mathbf{H}\|_F/M}$ makes $\mathbf{W}^H\mathbf{H}$ a scaled identity matrix and hence orthogonal. The optimal diagonal precoding, in this case, is to use the maximum power $\mathbf{V} = \sqrt{P_T}\mathbf{I}$ to maximize the SNR.[1] Hence, $\mathbf{H}_{eq}$ is an orthogonal matrix maximizing the SNR and thus solves the joint optimization. Thus, we have derived the optimal linear precoders and combiners for an uplink scenario.

IX. Numerical Evaluation

In this section, we evaluate the performance of the proposed algorithms using numerical simulations. The capacity improvements of position optimization are first evaluated along with their robustness to randomness due to the channel and UAV motion. Then, the convergence of Force Fields is evaluated under ideal and practical conditions along with other UAV positioning algorithms. The distance traveled per UAV for different swarm positions is then considered and compared to the derived upper bounds. Lastly, we evaluate the impact of position optimization on the capacity as we move to the massive MIMO regime with $M \gg N$.

[1]Note that for iterative algorithms, before convergence, $\mathbf{H}$ is not orthogonal and the proposed precoders and combiners are not necessarily optimal

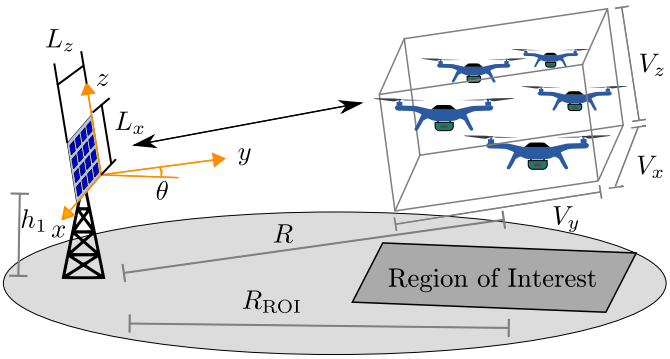

Fig. 4. In the simulation setup, the UAVs are initialized in a rectangular area. The GS is tilted towards the swarm.

A. Simulation Setup

We consider the simulation setup shown in Fig. 4. The GS consists of a URA having aperture $L_x = d_x M_x = 6$m and $L_z = d_z M_z = 6$m operating at a frequency of 5GHz. The large GS aperture reduces the distance traveled as shown in the derived upper bounds. However, an extremely large aperture is not practical. Unless otherwise stated, we use $M_x = 6$ and $M_z = 2$ making $d_x = 1$m and $d_z = 3$m. The GS is placed at a height $h_1 = 10m$, which is assumed to be higher than any surrounding buildings making a LOS path exist between the GS and swarm [5]. For UAVs deployed in a remote area, the GS can be adjusted to guarantee this condition. To account for non line-of-sight (NLOS) propagation paths, the channel is modeled as a Rician channel. The center of the region of interest is at a distance of $R_{\text{ROI}} = 2$km from the UAV swarm. For simplicity, the initial positions are randomly distributed in a rectangular parallelepiped having sides $V_x = 10$, $V_y = 300$, and $V_z = 300$. The elevation angle of the ground antenna used is $\theta = 0.043$rad making the average height of the swarm approximately 100m.

We consider the uplink scenario, where the UAVs are the transmitters. Channel estimation errors, when considered, are modeled using $\mathbf{H}_{\text{est}} = \mathbf{H} + \tilde{\mathbf{H}}$, where $\mathbf{H}_{\text{est}}$ is the estimated channel, and $\tilde{\mathbf{H}}$ is the channel estimation error. The estimation error is modeled as a matrix with independent complex Gaussian elements with zero mean and variance $\frac{1}{1+\text{SNR}\,T_\tau}$ where $T_\tau = 10$ is the number of training symbols [46]. The UAV motion errors, when considered, are modeled as an independent random Gaussian vector of size 3 having zero mean and a diagonal covariance matrix with a magnitude of 1m. This motion error vector is added to the positions of the UAVs before channel estimation [12].

Each UAV has a transmit power $P_T = 10$dBm and the bandwidth used is assumed to be 1MHz [47]. The noise power spectral density used is $N_0 = -174$dBm/Hz and the receiver has a noise figure N_F of 3dB, making the noise power equal to -111 dBm. We use the sum rate obtained when using linear minimum mean square error (LMMSE) combiner at the GS as a metric [9, 8.3.3]. The LMMSE

Authorized licensed use limited to: ASU Library. Downloaded on August 18,2023 at 20:13:23 UTC from IEEE Xplore. Restrictions apply.

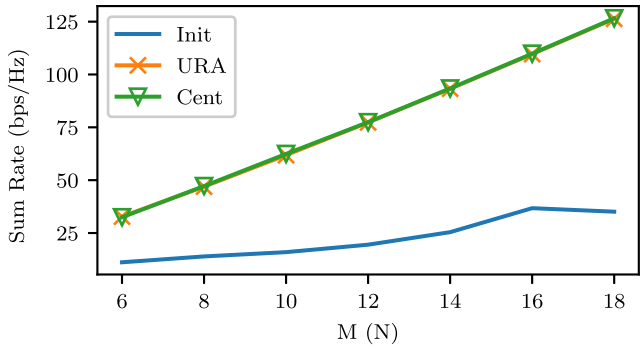

Fig. 5. As we increase the number of UAVs and GS antennas, Cent gives an equal sum rate to URA, which is higher than relying on the initial positions.

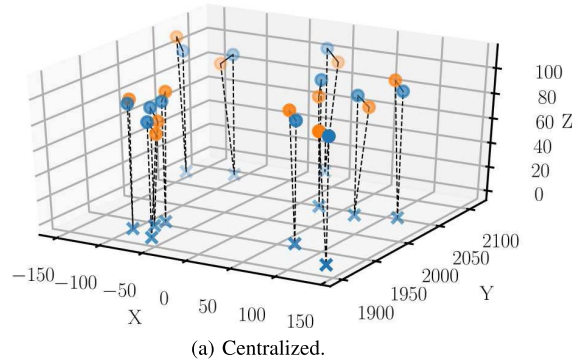

(a) Centralized.

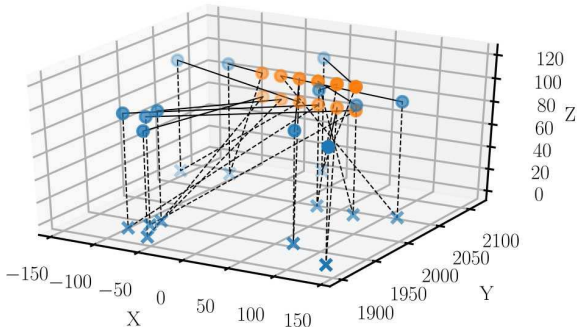

(b) URA.

Fig. 6. Blue dots represent the initial positions, orange dots the final positions of the UAVs. The dashes on the ground represent the point of interest. While URA and Cent optimize capacity, URA moves the UAVs significantly far from their points of interest.

combining vector w_n for UAV n is calculated using $\mathbf{w}_n = \left(N_0\ N_F\mathbf{I} + \sum_{i=0,i\neq n}^{N} \mathbf{h}_i^{[est]}\mathbf{h}_i^{[est]H}\right)^{-1} \mathbf{h}_n^{[est]}$, where $\mathbf{h}_n^{[est]}$ is the n-th column of the estimated channel. The signal-to-interference-and-noise ratio (SINR) of the n-th stream is given by $\text{SINR}_n = \frac{P_T|\mathbf{w}_n^H\mathbf{h}_n^{[c]}|^2}{N_0\ N_F + P_T\sum_{i=0,i\neq n}^{n}|\mathbf{w}_n^H\mathbf{h}_i^{[c]}|^2}$. Using the SINR of each stream, the sum rate is calculated using $\text{SR} = \sum_{n=0}^{N-1}\log\left(1+\text{SINR}_n\right)$

For comparison, we consider relying on the randomness of the initial UAV positions referred to as "Init". This is similar to what was proposed in [36], although we do not optimize the deployment region. We also consider positioning the UAVs using the technique proposed for traditional planar uniform-rectangular arrays (URAs) [31]. We also consider BF and GD from [12]. Although URAs were first proposed for fixed antenna arrays, they still can be used to maximize the capacity and along with uniform linear arrangements they have been proposed for UAVs [27], [32], [33], [35].

B. Performance Gains of Position Optimization

We start by demonstrating the performance gains that can be attained by optimizing the UAV swarm. We first consider the case of the swarm and GS having an equal number of antennas $M = N$ and we vary M_x. This is shown in Fig. 5. As the M_x increases, the sum rate of the optimized approaches (Cent and URA) increase linearly. This is expected from an optimized MIMO channel. However, this improvement comes at the cost of moving the UAVs from their initial positions. Unlike placing the UAV in a URA, our proposed approach minimizes the distance traveled. An example of a realization of random placement with $M_x = 6$ ($N = 12$) is shown in Fig. 6. The initial placements of the UAVs are shown in blue and is assumed to be above the points of interest shown as crosses at $z = 0$. For URA shown in Fig. 6b, UAVs need to travel 224m on average, which is far from the point of interest and might conflict with the objective of their deployment. On the other hand, for the centralized approach shown in Fig. 6a, each UAV needs to travel only an average distance of 20m from its initial position. This shows the limitation of relying on uniform placements.

After attaining the centrally optimized positions, we evaluate the robustness of our obtained solution against external disturbances. We consider the effects of NLOS propagation, channel estimation errors, and UAV motion errors. We vary the value of the Rician K Factor, and for each value, we simulate 100 random realizations of the Rician channel, localization errors, and channel estimation errors. We plot the mean of the sum rates in Fig. 7 with the standard deviation shown as error bars along with the single-user upper bound (UB) from (6). We see that for small values of the K-factor, the NLOS becomes dominant and both the optimized and non-optimized positions yield the same average capacity. As the LOS becomes more dominant and the K-factor increases, the optimized positions start approaching the capacity upper bound. The random initial positions, on the other hand, converge to a lower sum rate. This is what we expect since an unoptimized LOS MIMO channel is correlated. In practice, the LOS air-to-ground channel typically has a high K-factor. In channel measurement campaigns performed at a frequency of 5-GHz (C-band) for a LOS air-to-ground channel in near-urban and suburban environments, it was shown that the average K-factor was above 25dB [48, Table V].

C. Distributed Algorithms

Next, we evaluate the distributed algorithms performance in optimizing positions. URA approach and the centralized algorithm (Cent) are used as benchmarks. We compare Force Field (FF) against gradient descent (GD) and brute force (BF). For FF, we used $K_p = 0.3\frac{\min_n(\epsilon_n)S_x}{4\pi}$. The convergence results

Authorized licensed use limited to: ASU Library. Downloaded on August 18,2023 at 20:13:23 UTC from IEEE Xplore. Restrictions apply.

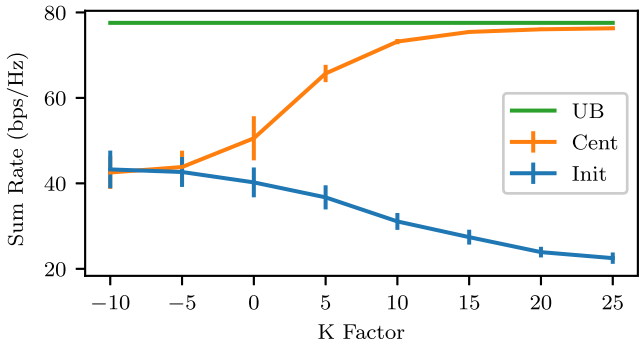

Fig. 7. Optimizing positions improves capacity for LOS dominant channel having a large K-factor. Simulation is done for the placement in Fig.6a and includes localization errors and channel estimation errors.

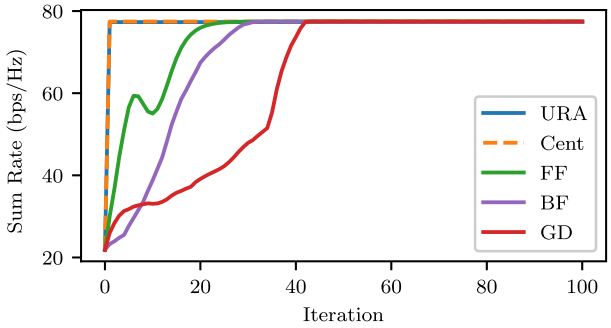

(a) Average sum rate

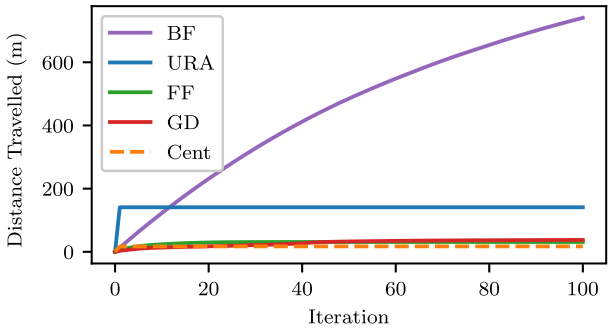

(b) Average distance traveled per UAV up to a given iteration. BF and URA were omitted for exceeding 100m.

Fig. 8. The sum rate and distance traveled for the ideal scenario.

for 100 iterations in an ideal scenario with $K = \infty$ are shown in Fig. 8. From Fig. 8a, we see that all the methods converge to the optimal sum rate. The average distance traveled per UAV up to a given iteration is shown in Fig. 8b with the curves for URA and BF omitted for exceeding 100m. This Figure along with Fig. 8a help characterize the tradeoff between attained capacity and the distance traveled. We can see that after the first two iterations with only 12m average traveled distance, the attained capacity is doubled. This shows that, using FF, significant gains can be attained with a few iterations and a limited traveled distance. Also while moving to optimize the capacity, the UAVs can work on their deployment tasks, hence FF does not impede on the deployment application.

Then, we evaluate the convergence of these methods under practical disturbances. Namely, we consider a K-factor

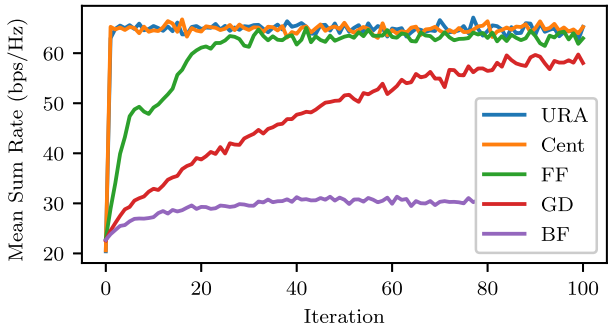

Fig. 9. The sum rate of distributed approaches under practical disturbances.

of 20dB along with channel estimation errors and localization errors added after each iteration. Also, in addition to the free space path loss, we consider log-normal fading with 3.2dB standard deviation applied independently to each UAV [48]. Using the same initial positions, 100 realizations of these random distortions were simulated. The average sum rate results are shown in Fig. 9. Compared to the ideal scenario, the sum rates even for URA and Cent are about 16% lower because fading affects the channel magnitude and hence the SNR per stream. However, we see that FF still converges to the sum rate bound attained by URA and Cent in about 30 iterations similar to the ideal scenario. GD, on the hand, takes more than twice the iterations to converge compared the ideal scenario due to the random changes in the channel magnitude affecting the gradients. Brute Force is severely impacted by the motion errors and does not converge [12]. Hence, our proposed FF is robust to practical disturbances expected in a swarm of UAVs and can attain the sum rate bound. Compared to GD and BF, FF requires only a fraction of the inter-swarm communications and is guaranteed to converge within a bounded distance in an ideal scenario.

D. Distance Traveled Per UAV

UAV applications have different tolerance for UAV translations from the initial positions. Hence, it important to evaluate the distance that each UAV needs to travel. To that end, we numerically evaluate the distance traveled by each UAV as a function of R. We consider 100 realizations, in which the UAVs are initialized randomly in a cube such that $V_x = V_y = V_z = 10$. The small cube guarantees that the UAVs are within $\mathcal{F}$ as we change the distance R. In Fig. 10, the solid lines show the mean distance traveled and the whiskers represent the range calculated over all realization and over the entire swarm. The upper bounds for Cent and FF derived in Propositions 2 and 3 respectively are plotted as dashed lines. We can see that the distance that the UAVs need to travel increases as R gets larger. This scaling is captured by our upper bounds, which can be used to estimate the worst case traveled distance. As expected, the distributed algorithm using only channel estimates requires a larger displacement than the centralized algorithm with perfect knowledge of the swarm initial positions. While we only show results for one center frequency and URA design, by using the upper bounds, verified in this

Authorized licensed use limited to: ASU Library. Downloaded on August 18,2023 at 20:13:23 UTC from IEEE Xplore. Restrictions apply.

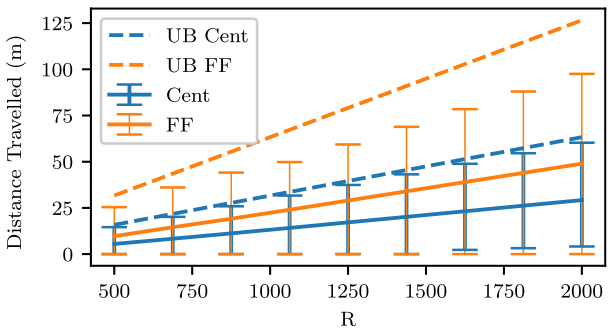

Fig. 10. The mean distance traveled by the swarm. The error bars represent the range.

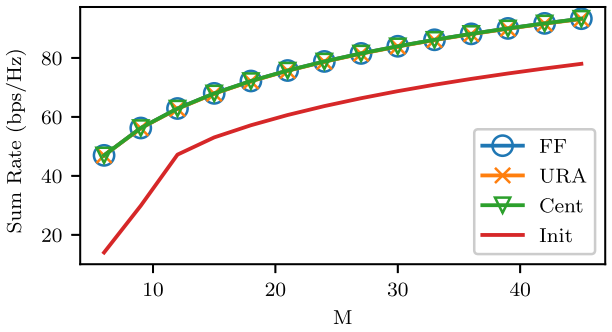

Fig. 11. The sum rate of different approaches as we move to the massive MIMO regime.

section, we can predict the effect of changing the URA design or the center frequency on the distance traveled.

E. Massive MIMO Evaluation

Now, we evaluate position optimization in the massive MIMO regime, where the number of GS antennas exceeds the number of UAVs $M \gg N$. Massive MIMO was shown to improve the capacity by increasing the number of GS antennas [49]. One might presume that increasing the number of GS antennas eliminates the need for position optimization. We show that this is not the case. We consider 8 UAVs and a GS with a fixed aperture such that $L_x = M_x d_x = 4$ and $L_z = M_z d_z = 6$. The ratio between antennas in the x and z direction was set to be $M_x/M_z = 2$ and the total number of GS antennas is increased [50]. From Fig. 11, we see that the optimized approaches provide a higher sum rate than the non-optimized as expected. But as the number of antennas increases the sum rate gap between both optimized and non-optimized approaches does not converge to zero. The suboptimal massive MIMO performance in a LOS channel was also observed and analyzed in [37, Sec. 4.3]. This indicates that even as the number of antennas increases, swarm optimization can provide significant improvements. One way to interpret this result is to consider the grid of optimal positions similar to the one shown in Fig. 2. For a fixed aperture massive MIMO setup (assuming the same x-z plane without loss of generality), the smallest distance between two optimal positions $\frac{S_x}{M_x}$ is constant and is equal to $\frac{\lambda R}{L_x}$. This means that by increasing the number of antennas, the optimal point density is the same. Hence, if the initial positions are far from any optimal ones, they will remain far as we increase M.

X. Conclusion

In this work, we optimized the placements of a UAV swarm to maximize the MIMO backhaul capacity starting from given swarm initial positions. We mathematically defined a set of UAV placements that orthogonalize the channel and maximize the MIMO capacity. The problem of minimizing the distance traveled to reach a placement in this set was formulated. An offline centralized solution was developed by relaxing the problem and decomposing it into two convex problems which were solved iteratively using block coordinate descent. We also proposed FF as a distributed iterative solution to this problem. FF requires sharing channel estimates only between neighbors and we derived the conditions for its convergence. Using numerical simulation, we have shown its robustness under channel and UAV induced disturbances. Upper bounds for the distance that UAVs need to travel using the centralized solution and force field were derived and numerically verified. Our approaches were shown to provide significant sum rate improvements while requiring only bounded displacements. The gains from our approach were shown to remain significant as we transition to the massive MIMO regime with far more ground station antennas than UAVs.

Appendix

A. Proof of Lemma 1

Let us define the scaled x and z translations, $x_n'' = \frac{x_n}{y_n}$ and $z_n'' = \frac{z_n}{y_n}$. We start by assuming that the solution is found on a uniform grid with respect of the scaled variables with dimensions M_x and M_z. The separation of the UAVs along this grid in the x and z planes is given by e_x and e_z, such that we can rewrite $x_n'' = i_c e_x$ and $z_n'' = j_c e_x$ for some integers $i_c \in \{0, \cdots, M_x - 1\}, j_c \in \{0, \cdots, M_z - 1\}$. Our objective, hence, becomes calculating the value of e_x and e_z. Starting from (11), we get

$$\mathbf{h}_l^H \mathbf{h}_k = \sum_{n=0}^{N-1} \exp\left(\frac{-j2\pi}{\lambda}\left((-i_l + i_k)d_x x_n'' + (-j_l + j_k)d_z z_n''\right)\right) \tag{45}$$

$$= \sum_{i_c=0}^{M_x-1} \sum_{j_c=0}^{M_z-1} \exp\left(\frac{-j2\pi}{\lambda}\left((-i_l + i_k)i_c d_x e_x + (-j_l + j_k)j_c d_z e_z\right)\right) \tag{46}$$

$$= \sum_{i_c=0}^{M_x-1} \exp\left(\frac{-j2\pi}{\lambda}\left((i_k - i_l)i_c d_x e_x\right)\right) \cdot \sum_{j_c=0}^{M_z-1} \exp\left(\frac{-j2\pi}{\lambda}\left((j_k - j_l)j_c d_z e_z\right)\right) \tag{47}$$

In (46), the summation over UAVs was rewritten as a summation over the x and z UAV grid positions. As is evident from equation (47), this summation is a product of two geometric

Authorized licensed use limited to: ASU Library. Downloaded on August 18,2023 at 20:13:23 UTC from IEEE Xplore. Restrictions apply.

sums and can therefore be simplified to

$$\frac{\sin\left(\frac{\pi M_x(i_k-i_l)d_x e_x}{\lambda}\right)}{\sin\left(\frac{\pi(i_k-i_l)d_x e_x}{\lambda}\right)}\frac{\sin\left(\frac{\pi M_x(j_k-j_l)d_z e_z}{\lambda}\right)}{\sin\left(\frac{\pi(j_k-j_l)d_z e_z}{\lambda}\right)}=0 \quad (48)$$

where the summation is set to 0 because of the orthogonality condition defined in (8). The orthogonality is achieved when $e_x=\frac{\lambda}{M_x d_x}$ and $e_z=\frac{\lambda}{M_z d_z}$. If we set y_n to be constant for all UAVs, we get the same condition derived for the optimal design of a parallel planar uniform rectangular arrays (URA) derived in [31], [51]. Hence, orthogonality is achieved when $x_n=i_n\frac{\lambda y_n}{M_x d_x}$ and $z_n=j_n\frac{\lambda y_n}{M_z d_z}$, where $n=i_n M_z+j_n$.

B. Proof of Proposition 1

The objective of (17) is monotonically increasing with respect to $(x'_{m,n})^2$. This objective is minimized by minimizing $(x'_{m,n})^2$. To prove that the optimal $f_{m,n}$ is within the set $\{-1,0\}$, we show that any value outside this set will correspond to a larger value of $(x'_{m,n})^2$.

Given that $0\le\tilde{x}_{m,n}\le S_x\epsilon_n$ and that $-\frac{1}{2}S_x\epsilon_n\le\delta_x S_x\epsilon_n\le\frac{1}{2}S_x\epsilon_n$ from (23), we get

$$-\frac{1}{2}S_x\epsilon_n\le\tilde{x}_{m,n}+\delta_x S_x\epsilon_n\le\frac{3}{2}S_x\epsilon_n \quad (49)$$

So, for any value of δ_x and $\tilde{x}_{m,n}$, using (25) the optimal value $\hat{f}_{m,n}$ can be calculated using

$$\begin{aligned}\hat{f}_{m,n}&=\underset{f_{m,n}\in\mathbb{Z}}{\operatorname{argmin}}(\tilde{x}_{m,n}+f_{m,n}S_x\epsilon_n+\delta_x S_x\epsilon_n)^2\\&=\begin{cases}0 & -\frac{1}{2}S_x\epsilon_n\le\tilde{x}_{m,n}+\delta_x S_x\epsilon_n<\frac{1}{2}S_x\epsilon_n\\-1 & \frac{1}{2}S_x\epsilon_n\le\tilde{x}_{m,n}+\delta_x S_x\epsilon_n\le\frac{3}{2}S_x\epsilon_n\end{cases}\end{aligned} \quad (50)$$

By substituting $\hat{f}_{m,n}$ to calculate the absolute translation $(\hat{x}'_{m,n})^2=\min_{f_{m,n}\in\mathbb{Z}}(x'_{m,n})^2$, we find that it is bounded by $(\hat{x}'_{m,n})\le(\frac{S_x\epsilon_n}{2})^2$. If $f_{m,n}$ is outside the set $\{-1,0\}$, we get a larger translation such that $(x'_{m,n})^2\ge\left(\frac{1}{2}S_x\epsilon_n\right)^2$. Hence, the optimal value of $f_{m,n}$ has to be within $\{-1,0\}$ and is given by (27).

C. Proof of Proposition 2

In the proof of Proposition 1, we showed that $(\hat{x}'_{m,n})^2\le(\frac{S_x\epsilon_n}{2})^2$ and similarly $(\hat{z}'_{m,n})^2\le(\frac{S_z\epsilon_n}{2})^2$. This holds for any value of the remaining variables. Hence, the translation made by UAV n is upper bounded by $\frac{\sqrt{S_x^2+S_z^2}}{2}\epsilon_n$.

D. Proof of Lemma 4

If K_p is sufficiently small, the phase unwrapping given by (38) retains the linearity of the measurements. Assuming UAV $n-1$ is fixed, x_{n-1} is constant across iterations, and we get

$$\begin{aligned}e_n[k]&=2\pi\left(\frac{x_n[k]}{\epsilon_n}-\frac{x_{n-1}}{\epsilon_{n-1}}\right)\frac{1}{S_x}-\psi_n\\&=2\pi\left(\frac{x_n[k-1]-K_p e_n[k-1]}{\epsilon_n}-\frac{x_{n-1}}{\epsilon_{n-1}}\right)\frac{1}{S_x}-\psi_n\\&=-2\pi\frac{K_p e_n[k-1]}{\epsilon_n S_x}+2\pi\left(\frac{x_n[k-1]}{\epsilon_n}-\frac{x_{n-1}}{\epsilon_{n-1}}\right)\frac{1}{S_x}-\psi_n\\&=\left(1-\frac{K_p 2\pi}{\epsilon_n S_x}\right)e_n[k-1]\end{aligned} \quad (51)$$

If $0<K_p<\frac{\epsilon_n S_x}{2\pi}$, the error will decrease in each iteration, and hence it will converge to zero. However, to avoid phase wrap errors when using (38) we need to guarantee that any transition does not exceed π, which is realized when $0<K_p<\frac{\epsilon_n S_x}{4\pi}$

REFERENCES

[1] H. Shakhatreh *et al.*, "Unmanned aerial vehicles (UAVs): A survey on civil applications and key research challenges," *IEEE Access*, vol. 7, pp. 48572–48634, 2019.

[2] M. Alzenad, A. El-Keyi, and H. Yanikomeroglu, "3-D placement of an unmanned aerial vehicle base station for maximum coverage of users with different QoS requirements," *IEEE Wireless Commun. Lett.*, vol. 7, no. 1, pp. 38–41, Feb. 2018.

[3] G. Hattab and D. Cabric, "Energy-efficient massive cellular IoT shared spectrum access via mobile data aggregators," in *Proc. IEEE 13th Int. Conf. Wireless Mobile Comput., Netw. Commun. (WiMob)*, Oct. 2017, pp. 1–6.

[4] M. Mozaffari, W. Saad, M. Bennis, Y.-H. Nam, and M. Debbah, "A tutorial on UAVs for wireless networks: Applications, challenges, and open problems," *IEEE Commun. Surveys Tuts.*, vol. 21, no. 3, pp. 2334–2360, 3rd Quart., 2019.

[5] J. Chen and D. Gesbert, "Efficient local map search algorithms for the placement of flying relays," *IEEE Trans. Wireless Commun.*, vol. 19, no. 2, pp. 1305–1319, Feb. 2020.

[6] E. Vinogradov, H. Sallouha, S. De Bast, M. M. Azari, and S. Pollin, "Tutorial on UAV: A blue sky view on wireless communication," *J. Mobile Multimedia*, vol. 14, no. 4, pp. 395–468, 2018.

[7] P. Popovsk *et al.*, "Scenarios, requirements and KPIs for 5G mobile and wireless system," Eur. Commission, Brussels, Belgium, Tech. Rep. EU FP7 INFSO-ICT-317669 METIS, D1.1, 2013.

[8] A. A. Khuwaja, Y. Chen, N. Zhao, M.-S. Alouini, and P. Dobbins, "A survey of channel modeling for UAV communications," *IEEE Commun. Surveys Tuts.*, vol. 20, no. 4, pp. 2804–2821, 4th Quart., 2018.

[9] D. Tse and P. Viswanath, *Fundamentals of Wireless Communication*. Cambridge, U.K.: Cambridge Univ. Press, 2005.

[10] A. Knopp, R. T. Schwarz, C. A. Hofmann, M. Chouayakh, and B. Lankl, "Measurements on the impact of sparse multipath components on the LOS MIMO channel capacity," in *Proc. 4th Int. Symp. Wireless Commun. Syst.*, Oct. 2007, pp. 55–60.

[11] H. Yan, S. Hanna, K. Balke, R. Gupta, and D. Cabric, "Software defined radio implementation of carrier and timing synchronization for distributed arrays," in *Proc. IEEE Aerosp. Conf.*, Mar. 2019, pp. 1–12.

[12] S. Hanna, H. Yan, and D. Cabric, "Distributed UAV placement optimization for cooperative line-of-sight MIMO communications," in *Proc. IEEE Int. Conf. Acoust., Speech Signal Process. (ICASSP)*, May 2019, pp. 4619–4623.

[13] A. Fouda, A. S. Ibrahim, Í. Güvenç, and M. Ghosh, "Interference management in UAV-assisted integrated access and backhaul cellular networks," *IEEE Access*, vol. 7, pp. 104553–104566, 2019.

[14] C.-C. Lai, C.-T. Chen, and L.-C. Wang, "On-demand density-aware UAV base station 3D placement for arbitrarily distributed users with guaranteed data rates," *IEEE Wireless Commun. Lett.*, vol. 8, no. 3, pp. 913–916, Jun. 2019.

[15] E. Krijestorac, S. Hanna, and D. Cabric, "UAV access point placement for connectivity to a user with unknown location using deep RL," in *Proc. IEEE Globecom Workshops (GC Wkshps)*, Dec. 2019, pp. 1–6.

[16] L. Bertizzolo, M. Polese, L. Bonati, A. Gosain, M. Zorzi, and T. Melodia, "MmBAC: Location-aided mmWave backhaul management for UAV-based aerial cells," in *Proc. 3rd ACM Workshop Millimeter-wave Netw. Sens. Syst. (mmNets)* New York, NY, USA: ACM, Oct. 2019, pp. 7–12.

[17] N. Tafintsev *et al.*, "Aerial access and backhaul in mmWave B5G systems: Performance dynamics and optimization," *IEEE Commun. Mag.*, vol. 58, no. 2, pp. 93–99, Feb. 2020.

[18] J. Pokorny *et al.*, "Concept design and performance evaluation of UAV-based backhaul link with antenna steering," *J. Commun. Netw.*, vol. 20, no. 5, pp. 473–483, Oct. 2018.

Authorized licensed use limited to: ASU Library. Downloaded on August 18,2023 at 20:13:23 UTC from IEEE Xplore. Restrictions apply.

[19] M.-J. Youssef, C. A. Nour, J. Farah, and C. Douillard, "Backhaul-constrained resource allocation and 3D placement for UAV-enabled networks," in *Proc. IEEE 90th Veh. Technol. Conf. (VTC-Fall)*, Sep. 2019, pp. 1–7.
[20] A. Fouda, A. S. Ibrahim, I. Guvenc, and M. Ghosh, "UAV-based in-band integrated access and backhaul for 5G communications," in *Proc. IEEE 88th Veh. Technol. Conf. (VTC-Fall)*, Aug. 2018, pp. 1–5.
[21] G. Geraci, A. Garcia-Rodriguez, L. G. Giordano, D. Lopez-Perez, and E. Björnson, "Supporting UAV cellular communications through massive MIMO," in *Proc. IEEE Int. Conf. Commun. Workshops (ICC Workshops)*, May 2018, pp. 1–6.
[22] A. Garcia-Rodriguez, G. Geraci, D. Lopez-Perez, L. G. Giordano, M. Ding, and E. Björnson, "The essential guide to realizing 5G-connected UAVs with massive MIMO," *IEEE Commun. Mag.*, vol. 57, no. 12, pp. 84–90, Dec. 2019.
[23] H. Huang, Y. Yang, H. Wang, Z. Ding, H. Sari, and F. Adachi, "Deep reinforcement learning for UAV navigation through massive MIMO technique," *IEEE Trans. Veh. Technol.*, vol. 69, no. 1, pp. 1117–1121, Jan. 2020.
[24] N. Rupasinghe, A. S. Ibrahim, and I. Guvenc, "Optimum hovering locations with angular domain user separation for cooperative UAV networks," in *Proc. IEEE Global Commun. Conf. (GLOBECOM)*, Dec. 2016, pp. 1–6.
[25] D. Xu, Y. Sun, D. W. K. Ng, and R. Schober, "Robust resource allocation for UAV systems with UAV jittering and user location uncertainty," Sep. 2018, *arXiv:1809.03706*. [Online]. Available: http://arxiv.org/abs/1809.03706
[26] D. Xu, Y. Sun, D. W. K. Ng, and R. Schober, "Multiuser MISO UAV communications in uncertain environments with no-fly zones: Robust trajectory and resource allocation design," May 2019, *arXiv:1905.10731*. [Online]. Available: http://arxiv.org/abs/1905.10731
[27] M. Mozaffari, W. Saad, M. Bennis, and M. Debbah, "Communications and control for wireless drone-based antenna array," Dec. 2017, *arXiv:1712.10291*. [Online]. Available: http://arxiv.org/abs/1712.10291
[28] L. Liu, S. Zhang, and R. Zhang, "CoMP in the sky: UAV placement and movement optimization for multi-user communications," Feb. 2018, *arXiv:1802.10371*. [Online]. Available: http://arxiv.org/abs/1802.10371
[29] X. Wang, W. Feng, Y. Chen, and N. Ge, "UAV swarm-enabled aerial CoMP: A physical layer security perspective," May 2019, *arXiv:1905.05449*. [Online]. Available: http://arxiv.org/abs/1905.05449
[30] F. Bohagen, P. Orten, and G. E. Oien, "Design of optimal high-rank line-of-sight MIMO channels," *IEEE Trans. Wireless Commun.*, vol. 6, no. 4, pp. 1420–1425, Apr. 2007.
[31] F. Bøhagen, P. Orten, and G. Øien, "Optimal design of uniform rectangular antenna arrays for strong line-of-sight MIMO channels," *EURASIP J. Wireless Commun. Netw.*, vol. 2007, no. 1, p. 12, Dec. 2007.
[32] W. Su, J. D. Matyjas, M. J. Gans, and S. Batalama, "Maximum achievable capacity in airborne MIMO communications with arbitrary alignments of linear transceiver antenna arrays," *IEEE Trans. Wireless Commun.*, vol. 12, no. 11, pp. 5584–5593, Nov. 2013.
[33] S. Hanna, E. Krijestorac, H. Yan, and D. Cabric, "UAV swarms as amplify-and-forward MIMO relays," in *Proc. IEEE 20th Int. Workshop Signal Process. Adv. Wireless Commun. (SPAWC)*, Jul. 2019, pp. 1–5.
[34] A. Pogue, S. Hanna, A. Nichols, X. Chen, D. Cabric, and A. Mehta, "Path planning under MIMO network constraints for throughput enhancement in multi-robot data aggregation tasks," in *Proc. IEEE/RSJ Int. Conf. Intell. Robots Syst. (IROS)*, Oct. 2020, pp. 11824–11830.
[35] P. Chandhar, D. Danev, and E. G. Larsson, "Massive MIMO for communications with drone swarms," *IEEE Trans. Wireless Commun.*, vol. 17, no. 3, pp. 1604–1629, Mar. 2018.
[36] A. T. Irish, F. Quitin, U. Madhow, and M. Rodwell, "Achieving multiple degrees of freedom in long-range mm-wave MIMO channels using randomly distributed relays," in *Proc. Asilomar Conf. Signals, Syst. Comput.*, Nov. 2013, pp. 722–727.
[37] H. Q. Ngo, E. G. Larsson, and T. L. Marzetta, "Aspects of favorable propagation in massive MIMO," in *Proc. 22nd Eur. Signal Process. Conf. (EUSIPCO)*, Sep. 2014, pp. 76–80.
[38] H. W. Kuhn, "The hungarian method for the assignment problem," *Nav. Res. Logistics Quart.*, vol. 2, nos. 1–2, pp. 83–97, Mar. 1955.
[39] S. Diamond and S. Boyd, "CVXPY: A Python-embedded modeling language for convex optimization," *J. Mach. Learn. Res.*, vol. 17, no. 83, pp. 1–5, 2016.
[40] D. P. Bertsekas, *Nonlinear Programming*. Belmont, MA, USA: Athena Scientific, 1999.
[41] J. Edmonds and R. M. Karp, "Theoretical improvements in algorithmic efficiency for network flow problems," *J. ACM*, vol. 19, no. 2, pp. 248–264, Apr. 1972.
[42] A. Domahidi, E. Chu, and S. Boyd, "ECOS: An SOCP solver for embedded systems," in *Proc. Eur. Control Conf. (ECC)*. Zurich, Switzerland: IEEE, Jul. 2013, pp. 3071–3076.
[43] F. A. Potra and S. J. Wright, "Interior-point methods," *J. Comput. Appl. Math.*, vol. 124, nos. 1–2, pp. 281–302, Jan. 2000.
[44] T. Haustein and U. Kruger, "Smart geometrical antenna design exploiting the LOS component to enhance a MIMO system based on Rayleigh-fading in indoor scenarios," in *Proc. 14th IEEE Pers., Indoor Mobile Radio Commun. (PIMRC)*, vol. 2, Sep. 2003, pp. 1144–1148.
[45] F. Golnaraghi and B. C. Kuo, *Automatic Control Systems*. New York, NY, USA: McGraw-Hill, 2017.
[46] B. Hassibi and B. M. Hochwald, "How much training is needed in multiple-antenna wireless links?" *IEEE Trans. Inf. Theory*, vol. 49, no. 4, pp. 951–963, Apr. 2003.
[47] Y. Zeng and R. Zhang, "Energy-efficient UAV communication with trajectory optimization," *IEEE Trans. Wireless Commun.*, vol. 16, no. 6, pp. 3747–3760, Jun. 2017.
[48] D. W. Matolak and R. Sun, "Air–ground channel characterization for unmanned aircraft systems—Part III: The suburban and near-urban environments," *IEEE Trans. Veh. Technol.*, vol. 66, no. 8, pp. 6607–6618, Aug. 2017.
[49] E. G. Larsson, O. Edfors, F. Tufvesson, and T. L. Marzetta, "Massive MIMO for next generation wireless systems," *IEEE Commun. Mag.*, vol. 52, no. 2, pp. 186–195, Feb. 2014.
[50] A. O. Martinez, J. O. Nielsen, E. De Carvalho, and P. Popovski, "An experimental study of massive MIMO properties in 5G scenarios," *IEEE Trans. Antennas Propag.*, vol. 66, no. 12, pp. 7206–7215, Dec. 2018.
[51] P. Larsson, "Lattice array receiver and sender for spatially OrthoNormal MIMO communication," in *Proc. IEEE 61st Veh. Technol. Conf.*, vol. 1, May 2005, pp. 192–196.

Samer Hanna (Graduate Student Member, IEEE) received the B.Sc. degree in electrical engineering and the M.Sc. degree in engineering mathematics from Alexandria University, Alexandria, Egypt, in 2013 and 2017, respectively. He is currently pursuing the Ph.D. degree with the University of California at Los Angeles, Los Angeles, CA, USA. His research interest includes the applications of machine learning in wireless communications and coordinated communications using unmanned aerial vehicles.

Enes Krijestorac (Graduate Student Member, IEEE) received the B.S. degree *summa cum laude*in electrical engineering from New York University at Abu Dhabi, Abu Dhabi, in 2018. He is currently pursuing the Ph.D. degree with the University of California at Los Angeles, Los Angeles, USA. His research interests include UAV assisted wireless communication, and modeling of wireless communication using machine learning and distributed computing systems.

Danijela Cabric (Fellow, IEEE) received the M.S. degree in electrical engineering from the University of California at Los Angeles (UCLA) in 2001 and the Ph.D. degree in electrical engineering from UC Berkeley in 2007. She is currently a Professor in electrical and computer engineering with the University of California at Los Angeles, Los Angeles. Her research interests include millimeter-wave communications, distributed communications and sensing for the Internet of Things, and machine learning for wireless networks co-existence and security. She received the Samueli Fellowship in 2008, the Okawa Foundation Research Grant in 2009, the Hellman Fellowship in 2012, the National Science Foundation Faculty Early Career Development (CAREER) Award in 2012, and the Qualcomm Faculty Award in 2020. She served as an Associate Editor for IEEE TRANSACTIONS OF COGNITIVE COMMUNICATIONS AND NETWORKING, IEEE TRANSACTIONS OF WIRELESS COMMUNICATIONS, IEEE TRANSACTIONS ON MOBILE COMPUTING, and *IEEE Signal Processing Magazine*. She also served as an IEEE ComSoc Distinguished Lecturer.

Authorized licensed use limited to: ASU Library. Downloaded on August 18,2023 at 20:13:23 UTC from IEEE Xplore. Restrictions apply.